recycling

MDPI

Article

Sustainable Valorization of Bovine–Guinea Pig Waste: Co-Optimization of pH and EC in Biodigesters

Daniela Geraldine Camacho Alvarez [1], Johann Alexis Chávez García [1], Yoisdel Castillo Alvarez [1,*] and Reinier Jiménez Borges [2,*]

[1] Environmental Engineering Career, Engineering Faculty, Universidad Peruana de Ciencias Aplicadas (UPC), Lima 15023, Peru
[2] Department of Mechanical Engineering, Faculty of Engineering, Universidad de Cienfuegos "Carlos Rafael Rodríguez", Cienfuegos 59430, Cuba
* Correspondence: pcigycas@upc.edu.pe (Y.C.A.); rjimenezborges@gmail.com (R.J.B.)

Abstract

The agro-industry is among the largest methane emitters, posing a critical challenge for sustainability. In rural areas, producers lack effective technologies to manage daily organic waste. Anaerobic digestion (AD) offers a circular pathway by converting waste into biogas and biofertilizers; however, its adoption is limited by inappropriate designs and insufficient operational control. Theoretical-applied research addresses these barriers by improving the design and operation of small-scale biodigesters, elevating pH and Electrical Conductivity (EC) from passive indicators to first-order control variables. Based on the design of a compact biodigester previously validated in the Chillón Valley and replicated in Huaycán under a utility model patent process (INDECOPI, Exp. 001087-2025/DIN), a stoichiometric $NaHCO_3$ strategy with joint pH–EC monitoring was formalized, defining operational windows (pH 6.92–6.97; EC 6200–6300 µS/cm and dose–response curves (0.3–0.4 kg/day for 3–4 day) to buffer VFA shocks and preserve methanogenic ionic strength. The system achieved stable productions of 370–462 L/day, surpassing the theoretical potential of 352.88 L/day calculated by Buswell's equation. A multivariable predictive model (linear, quadratic, interaction terms pH × EC, temperature, and loading rate) was developed and validated with field data: R^2 = 0.78; MAPE = 2.7%; MAE = 11.2 L/day; RMSE = 13.8 L/day; r = 0.89; residuals normally distributed (Shapiro–Wilk p = 0.79). The proposed approach enables daily decision-making in low-instrumentation environments and provides a replicable and scalable pathway for the safe valorization of organic waste in rural areas. The design consolidates the shift from reactive to proactive and co-optimized pH–EC control, laying the foundation not only for standardized protocols and training in rural systems but also for improved environmental sustainability.

Keywords: anaerobic digestion; compact biodigester; pH and electrical conductivity (EC); multivariable predictive model; rural sustainability

Academic Editor: Michele John

Received: 22 August 2025
Revised: 28 September 2025
Accepted: 30 September 2025
Published: 10 October 2025

Citation: Camacho Alvarez, D.G.; Chávez García, J.A.; Castillo Alvarez, Y.; Jiménez Borges, R. Sustainable Valorization of Bovine–Guinea Pig Waste: Co-Optimization of pH and EC in Biodigesters. *Recycling* **2025**, *10*, 190. https://doi.org/10.3390/recycling10050190

1. Introduction

The acceleration of population growth and urbanization has led to a substantial increase in organic waste generation globally, particularly from agricultural and animal production systems. Projections suggest this trend will continue to 2050, exacerbating Greenhouse Gas (GHG) emissions and adversely affecting soil and water resources [1,2]. The production of biogas from agro-industrial waste has been widely explored as an

energy and environmental solution in the context of the circular economy [3]. Agro-industrial waste consists of organic materials and by-products generated in agricultural production and processing, including both animal manure and lignocellulosic biomass, among others. Biogas projects can generally be associated with multiple substrate sources, such as liquid and solid waste from agribusiness, wastewater treatment plants that include anaerobic digestion in their system, directly from energy crops in agriculture, or from the capture of biogas produced in landfills [4]. Current practices in managing animal and agricultural waste often rely on inadequate disposal methods, which contribute significantly to methane emissions and environmental pollution. The transition towards sustainable waste management technologies, such as AD and composting, faces challenges related to required investments and technical development [5,6].

AD has matured in industrialized countries for valorizing organic waste at pilot and industrial scales. However, in developing countries, its adoption is still in early stages due to technological and infrastructural limitations, despite the large quantities of organic waste and energy demands that justify its expansion as a strategy for the circular economy and energy security [7,8]. In parallel, pre-treatments and co-digestion (AcoD) have been proposed to enhance biodegradability and biogas yield; at full scale, AcoD is used to stabilize digestate and mitigate inhibitions caused by volatile fatty acids (VFAs), improving the C/N balance and availability of micronutrients [9,10]. Nevertheless, operational gaps continue to explain instabilities, especially in small and rural plants [11].

AD stability is highly sensitive to operational and biochemical variables: pH, alkalinity, VFA, organic loading rate (OLR), hydraulic retention time (HRT), temperature, and C/N ratio. Poor control of these parameters leads to acidification episodes, loss of methanogenesis, and system shutdowns [12,13]. In cold climates or with inadequate insulation, thermal gradients and temperature variations exceeding 2–3 °C/h impair reaction kinetics and trigger system failures, demanding tailored design and operational solutions for rural environments [14,15].

Despite numerous reviews and guidelines, the dominant literature prioritizes temperature, pH, HRT, OLR, C/N, and VFA/TA (FOS/TAC) but rarely integrates EC as a control variable in full-scale plants, even though EC reflects the ionic strength and buffering capacity of the medium—parameters closely linked to resilience against acid accumulation and feed shocks [16,17]. Recent studies emphasize that EC plays a significant role in digestion and process stability, yet it is often overlooked or poorly monitored in practice [18,19]. This gap is particularly critical in domestic and rural biogas plants, where routine monitoring is limited to pH and temperature, and operation relies on manual mixing and scarce resources [20,21].

In previous studies, EC has often been omitted or treated as a secondary variable for several reasons. Primarily, the dominant literature has focused on well-established parameters such as pH, temperature, HRT, and OLR, which have historically been considered the main determinants of process stability and biogas production efficiency. EC, which reflects the ionic strength and buffering capacity of the medium, has received less attention because its mechanistic interpretation and control are more complex, especially in rural or small-scale systems where instrumentation for real-time measurement is limited.

Furthermore, the absence of replicable operating protocols that integrate active EC measurement and clear thresholds or operating windows has relegated EC to the role of a passive indicator rather than an active control variable. In fact, although EC is directly related to microbial resilience to acid accumulation and changes in organic load, its dynamic monitoring has not been sufficiently incorporated into conventional operational practices, especially in rural contexts where manual and low-tech methods predominate.

This research addresses this gap by uniquely integrating EC as a first-order control variable, together with pH. An operational framework based on dual pH–EC monitoring is formalized, defining specific operational windows (pH 6.92–6.97; EC 6200–6300 µS/cm) and dose–response curves for the stoichiometric dosing of $NaHCO_3$. This strategy allows for the buffering of volatile fatty acid shocks and preserves the methanogenic ionic strength necessary for the stability and productivity of the biodigester. Moreover, a multivariable predictive model is developed and validated that incorporates linear, quadratic, and interaction terms among EC, pH, temperature, and loading rate, achieving a high predictive capacity under limited technical resource field experimental conditions.

This proactive and co-optimized control paradigm surpasses the traditional reactive approach focused solely on pH, establishing EC as a crucial axis to maintain microbial homeostasis and buffering capacity, which are essential for resilience against variations in substrate composition and loading. Thus, the study not only presents a significant methodological advancement by incorporating EC as a controllable variable in rural and small-scale anaerobic digestion systems but also delivers replicable protocols and predictive tools that facilitate safer, more robust, and sustainable management of organic waste valorization in these contexts.

pH remains the "sentinel" parameter of methanogenesis (an optimal range of around 6.8–7.2), but keeping it stable requires preserving the buffering capacity (alkalinity) against VFA pulses. The technical literature recommends bicarbonate dosing as a corrective or preventive measure against acidification, supported by clear stoichiometric principles [22,23]. However, without measuring EC—an indicator of the ionic environment and the availability of HCO_3/CO_2—pH adjustments may be reactive and insufficiently robust against load and compositional variations, especially when co-substrates rich in potentially inhibitory compounds (proteins, lipids, phenolics, and monoterpenes) are used [24,25]. The most cited operational reviews describe control frameworks based on pH–VFA–TA and temperature–HRT–OLR–C/N, but they do not establish thresholds or monitoring routines for EC linked to alkalinity management, nor do they propose co-optimization protocols for pH–EC to stabilize the digester's ionic regime [26,27].

Experimental evidence confirms that instability caused by the accumulation of VFAs and spikes in OLR leads to drops in CH_4 production if system buffering variables are not properly controlled, particularly in co-digestion processes [28,29]. In developing countries, where AD could divert large organic waste flows from open dumping and generate distributed energy, reported plants are typically single-stage, mesophilic, and operating in monodigestion. Moreover, the number of plants described in scientific papers is lower than the number of installed systems, making it difficult to learn from real operational data and standardize best practices [30,31]. Economic barriers (capital and operational costs and equipment imports) and technical challenges (pre-treatment, source segregation, and variable control) also persist, slowing large-scale adoption [32,33].

The methodological gap is not only technological; the most widespread kinetic/predictive models (e.g., growth fittings and empirical models) are trained as being decoupled from online control routines and rarely include coupled operational variables (pH–EC–temperature –VS–OLR) with interaction terms, which limits their capacity to predict and manage the plant under real conditions. The research carried out in [14] in the Chillón Valley provided the scientific basis and a reproducible design-operation framework for rural biodigesters with structural improvements (inlet/outlet geometry, burial: 1.1 m, free volume: 30%, and passive insulation) and operational improvements (semi-continuous regime, induced agitation, management of HRT/OLR, and recirculation) that stabilize operation. In that study, the pH and EC variables were addressed as simple controls, with punctual and reactive actions under an essentially decoupled governance. Based on that experience, it was

identified in Huaycán that such an approach is insufficient; pH and EC behave as coupled and dominant state variables in the process's stability and productivity. Consequently, this research proposes a paradigm shift: moving from reactive monitoring to a proactive and co-optimized governance of pH–EC as the axes of operational control. It is worth noting that the biodigester design in question and its replica in Huaycán are also in the process of being patented as a utility model before INDECOPI (Exp. 001087-2025/DIN), which supports its transferability and standardization potential.

Therefore, the community lacks replicable operational protocols that integrate EC measurement, active alkalinity management, and predictive modeling validated in the field for small, rural plants. This work addresses that gap by proposing, for Huaycán, an operation architecture based on dual pH–EC control and its integration into a predictive model that incorporates linear, quadratic, and interaction terms among design and operation variables, with experimental validation under rural conditions and limited resources. In particular, the operationality of stoichiometric alkalinization with $NaHCO_3$ under joint pH–EC control: transforming acid–base/ionic balances into implementable control rules (target windows, dose–response curves, and limits to avoid osmotic stress).

This article presents several contributions, such as the following:

- Raising EC and pH to first-order control variables with clear thresholds.
- Validating a traceable multivariable predictive model for daily operational decision-making under field conditions.
- Delivering a replicable and scalable protocol for rural biodigesters aimed at the safe and sustainable valorization of organic wastes.

2. Materials and Methods

Establo Villa Asís (Avenida Andrés A. Cáceres, parcel 5; 17 km of Carretera Central, Huaycán, Ate, Lima) (Figure 1) is a productive and educational facility featuring milk milking, artisanal processing (cheese, yogurt, manjar, and ice cream), and guinea pig breeding modules. Additionally, it operates as a site for guided tours for schools and the general public, promoting circular economy and sustainability through the valorization of waste into energy and biofertilizers. The facility integrates dairy production and guinea pig modules, generating two main organic waste streams. Based on operational measurements and conservative estimates, the daily availability of waste (wet basis) is approximately 120–200 kg/d from guinea pigs—with a population 1500: 900 large (1.0–1.2 kg), 400 medium (0.5–0.7 kg), and 200 small (0–0.3 kg)—and 48 bovine heads: 11 lactating cows, 10 pregnant, 10 heifers, 10 young cows, 6 young bulls, and 1 breeding bull, producing around 1540–2050 kg/d. This quantification supports the sizing and operation of a wet anaerobic digestion system aimed at the energetic and agronomic valorization of these residues.

Figure 1. Geographical location of the Villa Asís biogas plant, Lima district.

2.1. Characterization of ORGANIC Matter

Table 1 summarizes the key physicochemical characteristics of the substrates used in this study: bovine manure and guinea pig manure. These parameters include elemental composition (carbon, hydrogen, oxygen, nitrogen, and sulfur) and solids content (total solids and volatile solids), which are critical indicators for evaluating the biodegradability and biogas production potential of the substrates. This elemental analysis of organic materials was carried out under the approach of Alvarez et al. (2025) [14]. Understanding these properties is essential to optimizing the co-digestion process, as variations in elemental and solid fractions influence microbial activity, substrate stability, and methane yield during anaerobic digestion.

Table 1. Physicochemical characteristics of the substrates.

Parameter	Units	Bovine Manure	Guinea Pig
C	%	47.70	46.20
H	%	6.63	7.12
O	%	34.52	32.78
N	%	2.06	2.32
S	%	0.95	0.81
TS	%	16.13	18.20
VS	%	14.47	16.55

In the context of improving small-scale biodigester designs for rural conditions, the characteristics of the system play a critical role in ensuring operational efficiency and biogas production. The biodigester analyzed in the case study by Alvarez et al. (2025) [14] features specific design parameters tailored to improve the anaerobic digestion process under typical rural constraints. Table 2 summarizes the key design specifications of this biodigester, including its volume, construction material, burial depth, inlet and outlet configurations, and the manual agitation system employed. These design features are fundamental to achieving stable mesophilic conditions, effective substrate mixing, and sufficient free gas volume for safe and efficient biogas accumulation.

Table 2. Design characteristics of the biodigester.

Parameter	Units	Value
Total biodigester capacity	L	1100
Working volume (effective load)	L	770 (70% of capacity)
Construction material	—	High-Density Polyethylene (HDPE)
Burial depth	m	1.10
Inlet angle	°	45
Inlet distance	m	3
Outlet height	cm	65
Outlet distance	m	2
Free gas volume (headspace)	%	30% of total volume
Agitation system	—	Manual, induced by feeding

2.2. Theory of Methane Potential Estimation

The Busswell equation [34], shown in Expressions (1) and (2), was used to determine the theoretical methane yield to empirically study substrates.

The literature reflects that the Buswell equation provides a sound theoretical basis for predicting methane production from the elemental composition of the substrate (C, H, O, N, S) but needs to be combined with empirical data kinetic adjustments, modeling

tools, and case-specific analysis to arrive at predictions that fit the operational reality of commercial-scale biodigesters [35–39].

$$C_nH_aO_bN_c + \left(n - \frac{a}{4} - \frac{b}{2} + \frac{3c}{8}\right)H_2O \longrightarrow \left(\frac{n}{2} + \frac{a}{8} - \frac{b}{4} + \frac{3c}{8}\right)CH_4 + \left(\frac{n}{2} - \frac{a}{4} + \frac{3c}{8}\right)CO_2 + cNH_3 \quad (1)$$

$$TMY = 100 \times 22.4 \times \left(\frac{\frac{n}{2} + \frac{a}{8} - \frac{b}{4} - \frac{3c}{8}}{12n + a + 16b + 14c}\right) \quad (2)$$

2.3. Variables' Measurement

The technological equipment used to monitor variables in the field was the same as that used in the previous study of the Chillón Valley [14] (Supplementary Materials). The Orion Star A211 pH Benchtop Meter (Thermo Scientific, Waltham, MA, USA) was used to measure the pH and temperature inside the biodigester. Temperature measurements were also obtained using an RTD (Resistance Temperature Detector, Xi'an Xinyuan Industrial Equipment Co., Ltd., Xi'an, China), which operates by detecting changes in the electrical resistance of materials like platinum, nickel, or copper. A commonly used RTD type, the Pt100, measures 100 ohms at 0 °C and adheres to international calibration standards such as IEC 60751 [40]. Additionally, biogas was measured using the JK/G1.6 m device (Qiantang District, Hangzhou, Zhejiang, China, which consists of four compartments separated by synthesized diaphragms. These compartments are periodically filled and emptied, with the diaphragms being moved by a gear connected to a crankshaft. This crankshaft actuates valves that control the gas flow. The measurement principle relies on pressure differences created by the gas flowing through the four chambers, causing the diaphragms to move back and forth. The volume of gas is transmitted to the meter via a series of mechanical linkages, and consumption is displayed through a counter, enabling accurate biogas measurement.

2.4. Theoretical Foundation: The Role of pH and $NaHCO_3$ in Anaerobic Digestion

pH is one of the most critical factors in anaerobic digestion, as it regulates enzymatic activity and the balance between the acidogenic and methanogenic phases. Methanogens (Methanobacterium, Methanosarcina) are extremely sensitive to acidification: their optimal range is between 6.8 and 7.2, while values below 6.5 drastically inhibit their methanogenic metabolism. Sodium bicarbonate acts as a buffering system due to its reversible dissociation into HCO_3^- and CO_2 [41,42]:

$$NaHCO_3 \leftrightarrow Na^+ + HCO_3^- \quad (3)$$

$$HCO_3^- + H^+ \leftrightarrow H_2CO_3 \leftrightarrow CO_2 + H_2O \quad (4)$$

This equilibrium neutralizes the protons released by the accumulation of VFAs during acidogenesis, increasing the total alkalinity (TAC) and stabilizing the pH within the methanogenic range.

2.5. Fitted Mathematical Model

For the development of the fitted mathematical model, an undefined logistic model (5) was used to describe the relationship between the bicarbonate dose ($NaHCO_3$) and the pH in the biodigester:

$$pH(D) = pH_{min} + \frac{pH_{max} - pH_{min}}{1 + e^{-k(D - D_{50})}} \quad (5)$$

where

- $pH_{min} = 4.50$ initial inhibition pH of the system).
- $pH_{max} = 6.86$ (asymptotic value reached in your data).
- $k = 5.00$ (response slope: sensitivity of pH to bicarbonate changes).
- $D_{50} = 0.384$ kg/day (dose to reach 50% of the maximum pH increase).

The best practices proposal for design allows us to propose a mathematical model to predict the daily biogas production and methane content as a function of variables related to the design and operation of the biodigester. The independent and dependent variables of the study [14] are presented in Table 3.

Table 3. Independent and dependent variables of the study.

Variable Type	Variable	Description	Unit
Independent	V_f	Free volume for biogas storage	%
	H_s	Outlet height of the digester	m
	$A_{in/out}$	Inlet and outlet angle of the digester	°
	T_r	Hydraulic retention time	d
	A_b	Manual agitation	Binary (0 or 1)
	C_d	Co-digestion proportion	%
	R_b	Biol recirculation	L/d
	$R_{MO:A}$	Organic matter ratio	kg/kg
Dependent	P_{biogas}	Daily biogas production	L/d
	Q_{CH_4}	Methane content in biogas	%

A multiple regression model, including linear, quadratic, and interaction terms (6), is used:

$$P_{\text{biogás}} = \beta_0 + \sum_{i=1}^{8} \beta_i X_i + \sum_{i=1}^{8} \beta_{ii} X_i^2 + \sum_{i<j}^{8} \beta_{ij} X_i X_j + \varepsilon \quad (6)$$

where

- β_0: Model intercept.
- β_i: Coefficients of linear terms.
- β_{ii}: Coefficients of quadratic terms.
- β_{ij}: Coefficients of interaction terms.
- ε: Random error term.
- X_i: Independent variables.

2.6. Extension and Validation of the Predictive Model: Integration of Operational and Biochemical Parameters

The proposed mathematical model (7) constitutes a robust extension of the original Valle del Chillón model, explicitly integrating construction variables (free volume, retention time, agitation, co-digestion ratio, and recirculation) together with operational and biochemical variables (fresh volatile solids, EC, pH, temperature, and their interactions). This formulation enables the prediction of daily biogas production under advanced experimental and operational scenarios, maximizing the model's fitting capacity and predictive scope (Table 4). This model can be extended based on these and other variables that are controlled.

Table 4. Independent and dependent variables used in this study.

Variable Type	Variable	Description	Unit
Independent	V_f	Free gas volume	%
Independent	T_r	Hydraulic retention time	days
Independent	A_g	Agitation (0/1)	–
Independent	C_d	Co-digestion proportion (% bovine manure)	%
Independent	R_b	Biofertilizer recirculation	L/d
Independent	VS_{fresh}	Volatile solids from fresh substrate fed	kg/d
Independent	Conductivity	EC of digestate	µS/cm
Independent	pH	Digestate pH	–
Independent	Temperature	Digestate temperature	°C
Dependent	$P_{biogás}$	Daily biogas production	L/d

$$\begin{aligned} P_{\text{biogas}}\,(\text{L/day}) = {} & \beta_0 + \beta_1 V_f + \beta_2 T_r + \beta_3 A_g + \beta_4 C_d + \beta_5 R_b \\ & + \beta_6 \text{VS}_{\text{fresh}} + \beta_7 \text{Conductivity} + \beta_8 \text{pH} + \beta_9 \text{Temperature} \\ & + \beta_{10}(\text{Conductivity} \times \text{pH}) + \beta_{11}(\text{VS}_{\text{fresh}} \times \text{Temperature}) \\ & + \beta_{12}(V_f \times T_r) + \beta_{13}(A_g \times C_d) \\ & + \beta_{14}(\text{Conductivity})^2 + \beta_{15}(\text{pH})^2 + \beta_{16}(\text{Temperature})^2 \\ & + \beta_{17}(\text{VS}_{\text{fresh}})^2 + \beta_{18}(\text{Conductivity} \times \text{Temperature}) \\ & + \beta_{19}(\text{pH} \times \text{Temperature}) \end{aligned} \tag{7}$$

2.7. Pseudo-R^2 in Logistic Regression Models

In logistic regression models, such as the one used to predict Q_{CH_4}, the traditional coefficient of determination (R^2) is not directly applicable due to the nonlinear categorical nature of the logistic function. Instead, alternative measures known as pseudo-R^2 are used, with McFadden's pseudo-R^2 being one of the most common and widely accepted [43–46].

McFadden's pseudo-R^2 is calculated as follows:

$$\text{pseudo-R}^2 = 1 - \frac{\ln \text{L}_{\text{model}}}{\ln \text{L}_{\text{null}}} \tag{8}$$

where

- $\ln \text{L}_{\text{model}}$: natural logarithm of the likelihood of the fitted model.
- $\ln \text{L}_{\text{null}}$: natural logarithm of the likelihood of the null model (a model that includes only the intercept).

Pseudo-values for R^2 in logistic regression are typically lower than R^2 values in linear regression and are not directly comparable. A pseudo-R^2 between 0.2 and 0.4 indicates a model with good predictive capacity.

2.8. Statistical Analysis

2.8.1. Mean Absolute Error (MAE)

The mean absolute error (MAE) (9) is a commonly used metric to quantify the average magnitude of errors between observed (real) and predicted (model) values, without considering their direction. It provides a straightforward measure of the accuracy of a predictive model, expressed as the average absolute difference between the actual data points and the model estimates. MAE is widely used in evaluating model performance due to its intuitive interpretation and sensitivity to individual prediction errors.

$$\text{MAE} = \frac{1}{n}\sum_{i=1}^{n}|y_{\text{real},i} - y_{\text{model},i}| \tag{9}$$

- $y_{\text{real},i}$: observed value.
- $y_{\text{model},i}$: predicted value.
- n: number of observations.

2.8.2. Root Mean Squared Error (RMSE)

The Root Mean Squared Error (RMSE) (10) is a widely used metric to measure the average magnitude of the errors between observed (real) and predicted (model) values. It provides a quadratic scoring rule that penalizes larger errors more than smaller ones, making it sensitive to outliers. RMSE is particularly useful for assessing the accuracy of predictive models, offering a clear numerical value that represents the standard deviation of the prediction errors.

$$\text{RMSE} = \sqrt{\frac{1}{n}\sum_{i=1}^{n}(y_{\text{real},i} - y_{\text{model},i})^2} \tag{10}$$

2.8.3. Mean Absolute Percentage Error (MAPE)

The Mean Absolute Percentage Error (MAPE) (11) is a statistical measure used to assess the accuracy of a predictive model by expressing the average absolute error as a percentage of the observed values. It provides a normalized metric that facilitates the comparison of errors across different datasets or scales. MAPE is particularly useful when interpreting the relative size of forecast errors, making it an intuitive and widely used criterion in model evaluation.

$$\text{MAPE} = \frac{100\%}{n}\sum_{i=1}^{n}\left|\frac{y_{\text{real},i} - y_{\text{model},i}}{y_{\text{real},i}}\right| \tag{11}$$

2.8.4. Coefficient of Determination (R^2)

The coefficient of determination, denoted as R^2 in Equation (12), is a commonly used statistical measure that quantifies the proportion of the variance in the observed data explained by the predictive model. It provides an indication of how well the model fits the data, with values closer to 1 representing a better fit. In regression analysis, R^2 serves as a key metric to evaluate the accuracy and explanatory power of the model by comparing the residual variance with the total variance of the observed values.

$$R^2 = 1 - \frac{\sum_{i=1}^{n}(y_{\text{real},i} - y_{\text{model},i})^2}{\sum_{i=1}^{n}(y_{\text{real},i} - \bar{y}_{\text{real}})^2} \tag{12}$$

2.8.5. Pearson Correlation Coefficient (r)

The Pearson Correlation Coefficient (r) (13) is a statistical measure that quantifies the strength and direction of the linear relationship between observed (real) and predicted (model) values. It ranges from -1 to 1, where values close to 1 indicate a strong positive correlation, values near -1 indicate a strong negative correlation, and values around 0 suggest no linear correlation. For a clearer and more meaningful interpretation, the strength of the correlation can be classified into categories such as very weak correlation ($|r| < 0.1$), weak correlation ($0.1 \leq |r| < 0.3$), moderate correlation ($0.3 \leq |r| < 0.5$), strong correlation ($0.5 \leq |r| < 0.7$), very strong correlation ($0.7 \leq |r| < 0.9$), and near perfect correlation ($0.9 \leq |r| \leq 1.0$). Such classification provides better insight into the predictive accuracy and reliability of the model than relying solely on the numeric values of -1, 0, or 1. This coefficient is widely used to assess the predictive accuracy and consistency of models by comparing predicted outputs with actual data.

$$r = \frac{\sum_{i=1}^{n}(y_{\text{real},i} - \bar{y}_{\text{real}})(y_{\text{model},i} - \bar{y}_{\text{model}})}{\sqrt{\sum_{i=1}^{n}(y_{\text{real},i} - \bar{y}_{\text{real}})^2 \sum_{i=1}^{n}(y_{\text{model},i} - \bar{y}_{\text{model}})^2}} \quad (13)$$

3. Results

The experimental system presented (Table 5) was originally designed for the co-digestion of bovine manure and guinea pig manure, aiming to maximize energy yield and operational stability through the synergy between both substrates. However, as part of a deliberate and scientific operational strategy, the process was initiated by first establishing a robust microbial base through the monodigestion of bovine manure, which acted as the main inoculum for the biodigester startup.

Table 5. Model validation data.

Date	Fresh VS (kg/d)	Conductivity (µS/cm)	pH –	Temp. (°C)	Actual Prod. (L/d)	Model Prod. (L/d)	Abs. Error (L/d)	Rel. Error (%)
1 July 2025	1.2075	6020	6.86	20.7	368.0	365.2	2.8	0.76
2 July 2025	0.6415	6220	6.91	22.7	374.0	389.7	−15.7	−4.20
3 July 2025	1.3585	6130	6.91	22.1	370.0	378.8	−8.8	−2.38
4 July 2025	0.6038	6360	6.95	24.0	376.0	369.3	6.7	1.78
5 July 2025	1.2830	6160	6.93	20.4	380.0	402.7	−22.7	−5.97
6 July 2025	0.6792	6230	6.97	21.3	374.0	406.8	−32.8	−8.77
7 July 2025	1.2075	6210	6.96	20.6	383.0	375.9	7.1	1.85
8 July 2025	0.6415	6050	6.93	20.6	435.0	413.5	21.5	4.94
9 July 2025	1.3585	6140	6.89	22.1	395.0	410.6	−15.6	−3.95
10 July 2025	0.6038	6120	6.93	21.8	426.0	399.2	26.8	6.29
11 July 2025	1.2830	6190	6.95	21.7	404.0	420.1	−16.1	−3.99
12 July 2025	0.6792	6120	6.94	20.0	402.0	421.2	−19.2	−4.78
13 July 2025	1.2075	6240	6.94	21.3	433.0	427.8	5.2	1.20
14 July 2025	0.6415	6240	6.95	20.9	431.0	421.9	9.1	2.11
15 July 2025	1.3585	6220	6.95	22.7	416.0	421.4	−5.4	−1.30
16 July 2025	0.6038	5940	6.91	20.7	401.0	400.6	0.4	0.10
17 July 2025	1.2830	6080	6.95	20.7	412.0	418.3	−6.3	−1.53
18 July 2025	0.6792	6160	6.95	21.7	415.0	429.4	−14.4	−3.47
19 July 2025	1.2075	6100	6.94	21.6	438.0	447.3	−9.3	−2.12
20 July 2025	0.6415	6120	6.95	21.7	462.0	455.4	6.6	1.43

The values presented in Table 6 correspond to the theoretical maximum potential for biogas and methane production. These were estimated by applying the Buswell and Mueller (1952) equation based on the elemental composition of each substrate, considering the actual contribution of VS in the fresh Organic Matter (OM). It is important to highlight that these values do not represent the expected real operational performance in anaerobic digestion systems at laboratory or industrial scale, but rather the maximum biochemical potential, which, depending on the system and operating regime, may achieve around 30% efficiency.

Table 6. Estimated theoretical production of methane and biogas for 1 kg of substrate, calculated using the Buswell equation under total degradation (100%).

Type of Digestion	CH_4 (L/kg OM)	CH_4 (L/kg VS)	Biogas (L/kg OM)	Biogas (L/kg VS)
Monodigestion (bovine manure)	19.33	133.6	32.20	222.5
Monodigestion (guinea pig)	43.14	260.7	71.90	434.4

The results obtained show that the theoretical biogas potential per kg of OM is substantially lower than the value reported per kg of VS, due to the low fraction of VS in the fresh OM of both substrates. This methodological approach is not only consistent with experimental practice and the recommendations of IEA Bioenergy and the international

literature, but also allows direct comparison with the actual production observed in the system, which is based on the daily feeding of OM.

Based on the conversion factors determined in this research (yields per VS for cattle and guinea pig) and biomass availability, the combined theoretical methanogenic potential amounts to approximately 28.2–39.3 m^3 CH_4/day, equivalent to approximately 44–66 m^3 biogas/d (assuming 50–60% CH_4). Figure 2 shows the daily biogas production obtained for different bovine manure/guinea pig substrate ratios. Although the 30:70 ratio offers the maximum theoretical and experimental yield, the selection of the 70:30 mixture for the biodigester operation is supported by the analysis of the C/N ratio obtained from the actual elemental analysis of the substrates.

According to laboratory data, the C/N ratio of the 70:30 mixture is 22.1, while in the 30:70 mixture, it decreases to 20.8. Both proportions fall within the optimal range considered for anaerobic digestion (15–30); however, higher values within this range are associated with greater stability and a lower risk of ammonia inhibition, which is especially relevant when increasing the fraction of guinea pig manure richer in nitrogen.

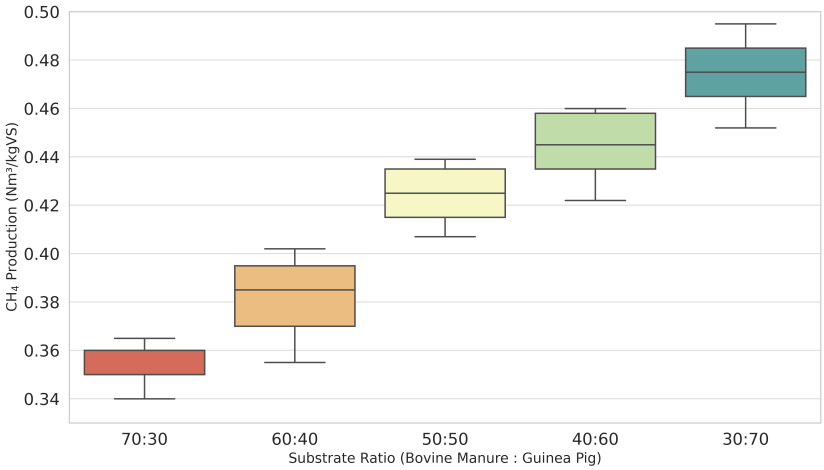

Figure 2. Distribution of biogas production for different substrate proportions (bovine manure/guinea pig).

For this reason, the 70:30 mixture is prioritized, sacrificing a fraction of the potential biogas yield in favor of a more robust, stable, and safe, long-term operation. This decision aligns with literature recommendations to maintain microbiological stability and avoid inhibition episodes in biogas plants.

Therefore, the choice is based on the balance between maximizing methanogenic potential and ensuring safe operating conditions, grounded in the real chemical characterization of the substrates and the fundamental principles of anaerobic digestion.

3.1. Monitoring of Key Operational Variables

Temperature and pH

Figure 3 illustrates the daily simultaneous monitoring of the pH and temperature in the biodigester during the initial operation phase (March-April), an essential approach to understanding microbial dynamics and system stability. From the startup, a progressive decrease in pH is observed, reaching minimum values close to 4.8, indicative of severe acidification attributable to the accumulation of VFAs during the accelerated acidogenic phase. Meanwhile, the system temperature fluctuates within a mesophilic range (25–32 °C), with moderate variations but without reaching critical values for microbial activity.

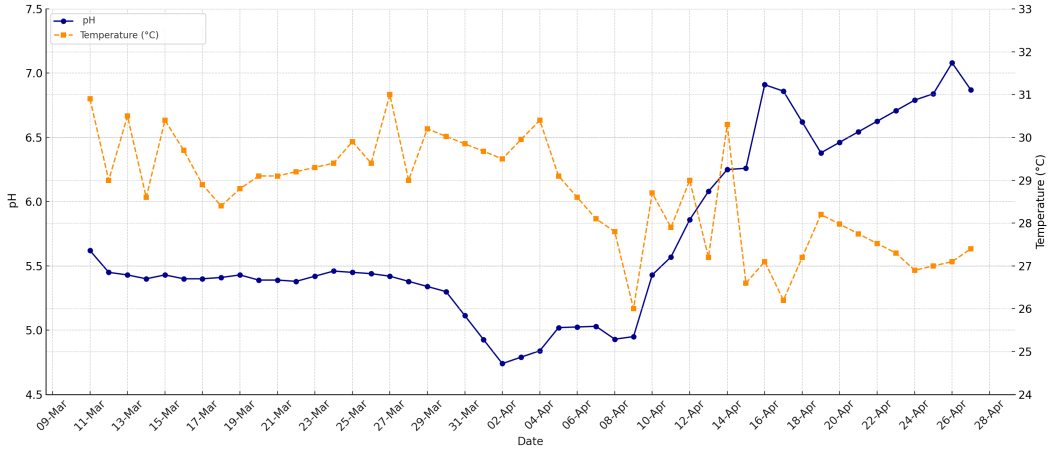

Figure 3. Simultaneous evolution of pH and temperature in the biodigester during the initial phase.

It is important to highlight that although the temperature was maintained within an adequate operational range for anaerobic digestion, the extreme acidification of the pH became the main limiting factor, jeopardizing methanogenic activity. This behavior evidences that, under the rural design conditions and feeding employed, temperature alone does not guarantee process stability if pH is not rigorously controlled.

The simultaneous monitoring of both variables allowed early identification of the need for intervention (alkaline correction), demonstrating that success in biogas production depends on a holistic management of critical parameters, and that pH control is fundamental for the survival and optimal performance of methanogenic archaea, even under apparently favorable thermal conditions.

Figure 4 shows the daily temporal evolution of pH and EC during the initial operation phase (March–April) of the biodigester, where a critical early acidification phenomenon was observed. The system experienced a progressive pH drop below 5.0, accompanied by fluctuations in EC, indicating accumulation of VFAs and an imbalance in the system's buffering capacity.

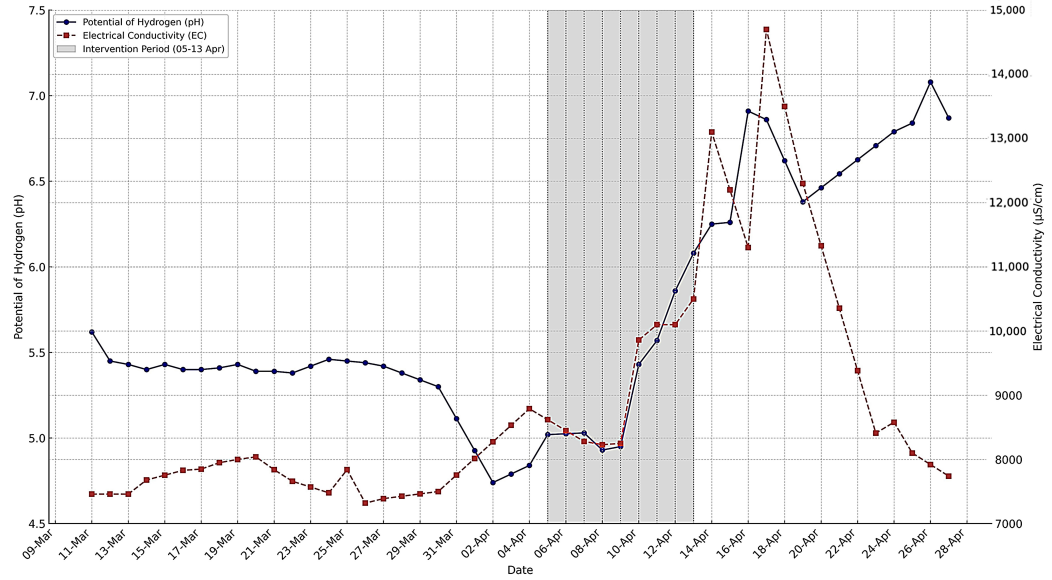

Figure 4. Simultaneous evolution of pH and EC in the biodigester during the initial phase.

During the initial process stage, Figure 4 shows a sustained pH decrease below 5.0, accompanied by low and stable EC, reflecting an accelerated acidogenesis scenario in which

the accumulation of volatile fatty acids exceeds the buffering capacity of the system, generating a strongly inhibitory environment for methanogenesis. The strategic intervention, indicated in the shaded area (April 5–13) through controlled addition of $NaHCO_3$, produces an immediate effect: pH quickly rises above the critical threshold of 6.5, restoring the optimal range for methanogenic archaea, while EC experiences a transient peak, indicative of increased buffering capacity and ionic availability in the medium. After the intervention, a progressive stabilization of pH around optimal values (6.8–7.2) is observed along with a gradual decrease in EC, confirming both the effective neutralization of accumulated acids and the functional reactivation of the methanogenic community and the restoration of biogas production, validating the critical importance of monitoring and timely intervention in anaerobic digestion systems.

3.2. Interpretation: Evolution of pH and Bicarbonate Dose

Proper pH control in a biodigester is essential to maintain the stability of the anaerobic digestion process and to ensure efficient biogas production. In this context, the controlled addition of $NaHCO_3$ acts as a buffering agent to neutralize the acidification caused by the accumulation of volatile fatty acids. The following interpretation details the different phases observed in the evolution of pH and the applied bicarbonate dose during the experimental operation, highlighting the system's response to chemical interventions and their impact on microbiological stability (Figure 5).

3.2.1. Initial Phase (04/05—pH ≈ 5.02)

- The system showed strong initial acidification due to rapid hydrolysis and acidogenesis, with an inhibitory pH (<6.0) that halted methanogenic activity.
- The initial addition of 300 g of $NaHCO_3$ began to partially buffer the acidity, evidenced by a progressive increase to pH 5.8 within 48 h.

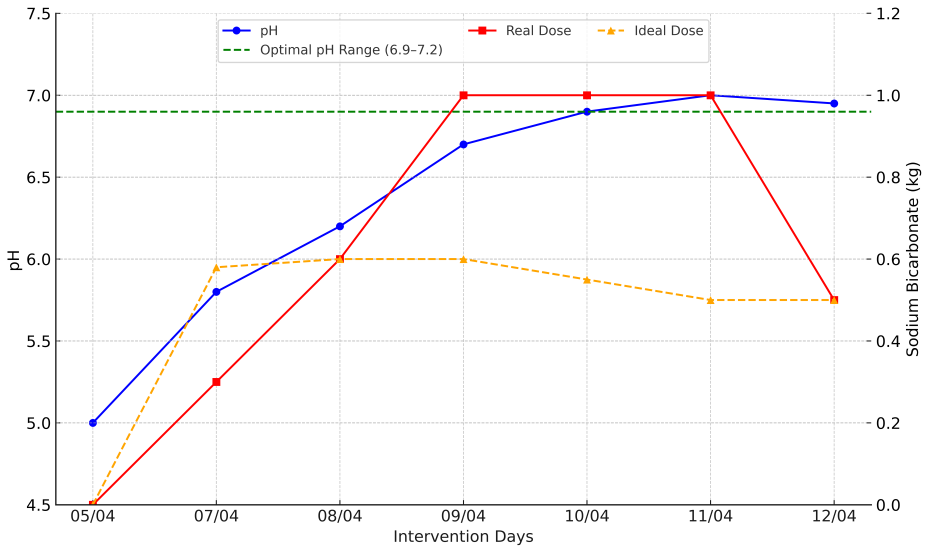

Figure 5. Severe acidification and recovery intervention phase.

3.2.2. Controlled Overcorrection (04/07–04/11)

- Successive doses of 0.3 to 1.0 kg/day of $NaHCO_3$ were added.
- This produced an exponential rise in pH, reaching the optimal range (6.9–7.0) in just 96 h, significantly faster than the standard rate reported in the literature (5–7 days with stoichiometric dosing).

- At this point, the bicarbonate concentration exceeded the calculated ideal dose by 41%, which increased total alkalinity and accelerated the neutralization of VFAs (acetic, propionic, and butyric acids).

3.2.3. Stabilization (04/12)

- The blue line (actual pH) shows a plateau trend at pH ≈ 6.95, while the red line (actual dose) indicates that recent $NaHCO_3$ additions were higher than the estimated stoichiometric requirement.
- This bicarbonate overfeeding, although not producing immediate negative effects, increased the EC (above 13,000 μS/cm in subsequent days), indicating ionic accumulation and possible osmotic stress if maintained long-term.

The rapid recovery of pH to the optimal range for methanogenic activity significantly favored the reactivation of the microbial consortium responsible for methane production, which was subsequently reflected in a marked increase in biogas generation, exceeding 400 L/day. From an acid–base balance perspective, it is likely that the ratio of VFAs to total alkalinity (TAC), considered a proxy for operational stability, decreased from critical values above 0.5 to stable ranges below 0.3, correlating directly with the alkalinization induced by the bicarbonate addition. However, excessive use of $NaHCO_3$ may have exceeded the required proton absorption capacity, raising alkalinity without providing additional pH benefits. Quantitatively, the intensive bicarbonate correction was effective, achieving a pH increase from 5.02 to 6.95 in just seven days, three days earlier than expected with a standard correction. This rapid stabilization was accompanied by overdosing, implying an excess of approximately 41%, since the actual cumulative dose was around 4.9 kg compared to an estimated ideal dose of 3.4 kg. Although this excess accelerated the system's recovery, it generated a secondary increase in EC that should be carefully monitored to avoid possible osmotic effects and to ensure a controlled transition to a full and stable methanogenic phase.

3.3. Biogas Production Control

This section compares the theoretical methane production estimated using the Buswell equation, the model proposed by [14], and the experimental values obtained in monodigestion and co-digestion systems. The temporal dynamics of daily methane production were analyzed as a function of substrate composition and operating conditions, with the aim of evaluating the degree of approximation to the estimated theoretical values. This analysis demonstrates the effectiveness of the operational strategies applied and clarifies the influence of substrate type and critical parameter management on the actual performance of rural-scale biodigesters.

Figure 6 shows the temporal evolution of daily methane production in the bovine manure monodigestion system, using this substrate as the base inoculum after recovery of the biodigester. The dashed red line corresponds to Buswell's theoretical potential. It is important to note that Buswell's equation provides a specific yield (L CH_4/kg VS) and not absolute production. In order to compare it directly with the experimental data expressed in L/day, this value was converted to absolute production by multiplying the theoretical yield (286 L CH_4/kg VS) by the average volatile solids feed (≈0.90 kg VS/day), obtaining ≈258 L CH_4/day. The blue line represents the theoretical production reported in [14] of 265 L/day, while the orange curve corresponds to the experimental production measured in the field.

The results show that, after restoring optimal pH and buffer capacity conditions, the system reached a stable production pattern, with measured values frequently exceeding the reference of 258 L CH_4/day and reaching peaks above 400 L/day. The standardized values presented in Table 6 are, again, expressed in CH_4 (L/kg VS) and derived from normalized

field data. This does not mean that Buswell's theoretical potential has been exceeded, but rather that absolute volumetric production increased as a result of the organic load applied, which varied between 0.60 and 1.35 kg VS/day.

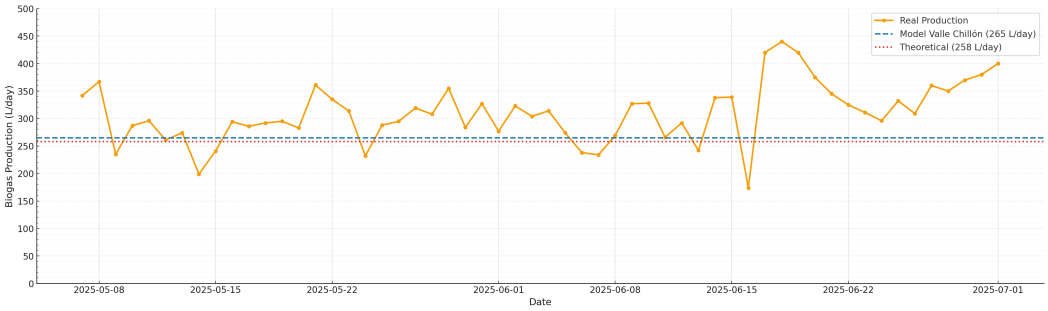

Figure 6. Actual biogas production compared to theoretical production (258 L CH_4/day).

This outstanding behavior is attributable to the combination of strict pH control and deliberate adjustment of EC during startup through alkaline intervention with sodium bicarbonate. This operational strategy quickly restored the optimal environment for methanogenesis, accelerating the adaptation of the microbial community and favoring the efficient conversion of organic matter into biogas, even under rural conditions with manual stirring induced only by feeding. This comparison was made on the basis of field measurements, rather than against the actual stoichiometric maximum. Furthermore, without direct data on CH_4 composition, it is impossible to say whether the observed increase represents a net gain in methane or simply additional CO_2. Comparison based solely on field measurements, rather than against the actual stoichiometric maximum, introduces a significant limitation in assessing the efficiency of the biogas production process. Field measurements may be subject to inherent variability in operating conditions and inaccuracies in data collection, which could distort the interpretation of full-scale performance.

Furthermore, the absence of direct data on CH_4 composition creates significant uncertainty regarding the nature of the observed increase. Without specific analysis of the methane content, it is not possible to discern whether the increase corresponds to a genuine net gain in methane production, which is the energetically valuable component of biogas, or whether it is simply an increase in the concentration of carbon dioxide CO_2, which does not contribute energy and may be indicative of suboptimal processes or even energy losses.

These limitations highlight the need for more detailed and quantitative analyses of biogas composition, as well as an experimental design that includes stoichiometric reference parameters for a more accurate assessment of the process. Only with this data will it be possible to optimize and validate predictive models with greater certainty and practical applicability.

Figure 7 shows the evolution of the actual daily biogas production (orange line) following the operational transition to co-digestion of bovine manure and guinea pig manure in a 70:30 ratio, compared with the estimated theoretical potential (red dashed line, 352.88 L/day) calculated according to the Buswell equation and the real physicochemical characteristics of the substrates. The blue line represents the theoretical production determined in [14] of 265 L/day. A quantitative leap in biogas production is observed compared to the monodigestion stage, with actual values consistently exceeding the theoretical potential on most monitored days, reaching peaks above 440 L/day. This outstanding performance confirms the metabolic synergy of co-digestion, where the substrate mixture improves the nutritional balance and favors microbial diversity, increasing the rate of organic matter conversion into biogas.

It is worth noting that this result was made possible thanks to the operational strategy of establishing a robust base inoculum (bovine manure monodigestion) before progressively introducing the complementary substrate (guinea pig manure), as well as the active management of pH and EC. Timely intervention with sodium bicarbonate and rigorous monitoring allowed for maintaining optimal conditions for methanogenesis, minimizing inhibition risks, and stabilizing the system, even in a rural context with limited resources and manual stirring.

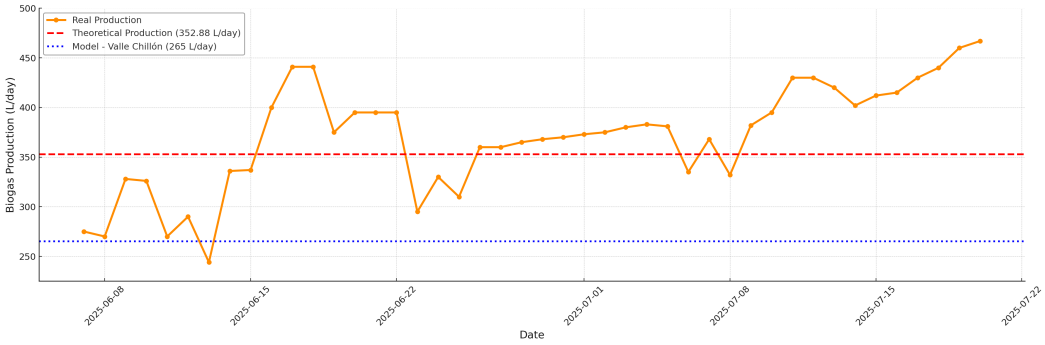

Figure 7. Actual biogas production compared to theoretical production (352.88 L CH_4/day).

Figure 8 shows a saturation behavior, typical of systems with limited buffering capacity, where the pH responds to increases in the bicarbonate dose until reaching a stable maximum level. In this case, the optimal pH range for methanogenic activity (6.9–7.2) is achieved with a dose close to 0.4–0.5 kg/day of bicarbonate. Although the actual additions made were higher than this saturation dose, between 0.8 and 1.0 kg/day, this overdose allowed for accelerated pH recovery, reaching the desired values in less time. This trend indicates that while doses higher than necessary do not further increase the pH, they do contribute to a faster system response to restore optimal conditions, which is beneficial for the startup and stability of the biodigester.

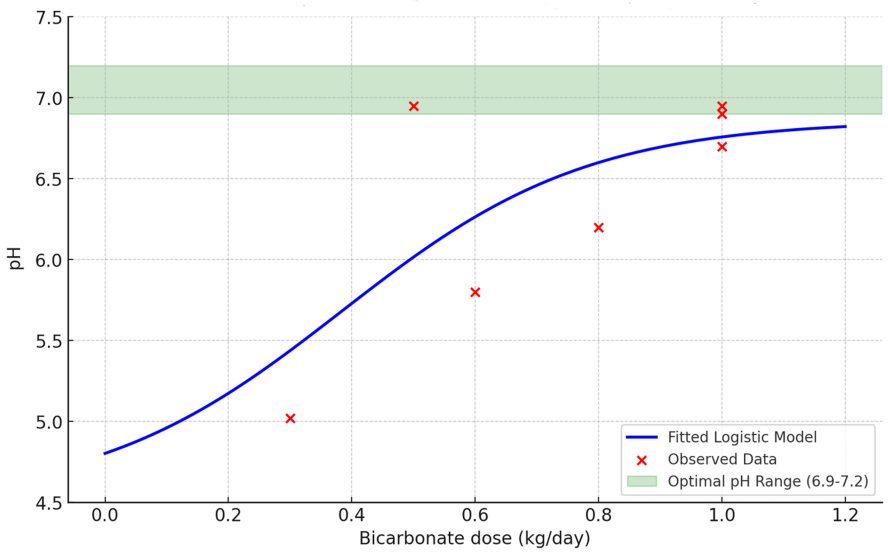

Figure 8. Logistic model fit: Bicarbonate dose vs. pH in biogas digester.

3.4. System Sensitivity

The pH response to the $NaHCO_3$ dose is a key aspect for the efficient and stable control of the biodigester. Analyzing the system's sensitivity $\left(\frac{d\text{pH}}{d\text{D}}\right)$ (14) allows for determining the optimal amount of bicarbonate needed to quickly restore the pH range favorable for methanogenic activity, avoiding both prolonged acidification and unnecessary overdosing.

Based on the obtained logistic fit, relevant scientific conclusions are drawn that validate the applied strategy and offer recommendations for future corrections to optimize the process from a thermodynamic and biological perspective. Near the D_{50} dose, the rate of pH change reached its maximum value, which can be approximated as

$$\frac{d\text{pH}}{d\text{D}} \approx 1.57 \frac{\Delta\text{pH}}{\text{kg NaHCO}_3} \quad (14)$$

This means that in this region, every 100 g of $NaHCO_3$ added increased the pH by approximately 0.16 units. However, above doses of 0.6–0.7 kg/day, the slope of the curve flattens, indicating that adding more bicarbonate produces diminishing returns.

From these observations, several scientific conclusions arise. First, the logistic curve validates the strategy applied: although a slight overdose of bicarbonate was administered, this led to a reduction in the duration of inhibition. For future corrections, a sequential dose of 0.3–0.4 kg/day for 3–4 days would be sufficient to reach the optimal pH range without excess. Finally, this fit demonstrates thermodynamic and biological coherence, as the pH behavior follows the neutralization kinetics controlled by the system's alkalinity and the CO_2/HCO_3^- equilibrium.

3.5. *Effect of pH on Biogas Production During the Inoculation and Co-Digestion Phases*

Figure 9 illustrates the relationship between pH and the daily biogas production (L/day) in two distinct operational phases: the inoculum stabilization phase using cattle manure as the sole substrate, and the co-digestion phase, which integrates guinea pig manure as a co-substrate.

During the initial inoculum phase, the system undergoes microbial adaptation and colonization, using exclusively bovine manure as substrate. In this stage, biogas production was moderate, stabilizing below 350 L/day. A notable decrease in pH was observed at the start of the process due to the accumulation of volatile fatty acids (VFAs), a common phenomenon in newly started anaerobic digesters. This acidification posed a threat to methanogenic activity, especially as pH approached levels below 6.8, where methanogenesis is progressively inhibited.

To counteract this acidic imbalance, $NaHCO_3$ was strategically applied as a chemical buffer. This intervention effectively stabilized the pH within the favorable operational range for methanogenic archaea, typically between 6.8 and 7.2, enabling the transition to a stable and active inoculum.

After system stabilization, the co-digestion phase began with the addition of guinea pig manure, a substrate characterized by higher organic load and nutrient density. This led to a significant increase in biogas production, with daily output exceeding 450 L/day. The co-digestion strategy not only improved substrate diversity but also enhanced the C/N ratio and promoted synergistic microbial interactions, key factors for increasing process efficiency.

It is noteworthy that both phases exhibit a quadratic relationship between pH and biogas production, highlighting the existence of an optimal pH range. Beyond this range, an increase in pH does not correlate with higher gas production, emphasizing the importance of precise pH management.

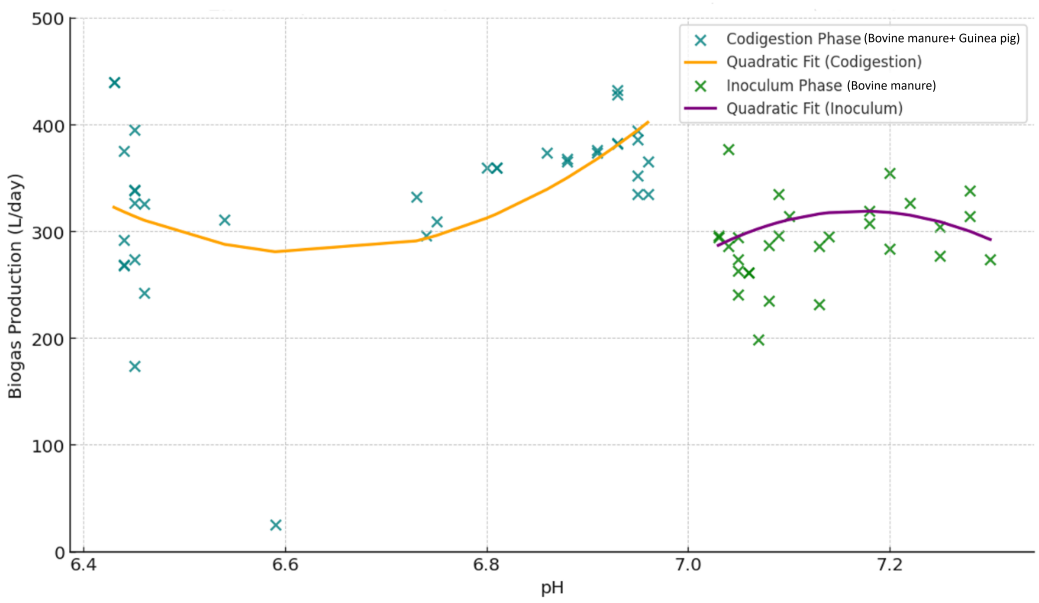

Figure 9. Effect of pH on biogas production vs. co-digestion phases.

3.6. Multivariable Analysis of the Synergistic Impact of EC and pH on Biogas Production

Figure 10 clearly shows that biogas production does not respond linearly to an increase in EC, but rather exhibits a parabolic behavior with a clearly defined maximum. The optimal production point is located around 6300 µS/cm. Up to this value, increasing EC favors methanogenic activity by improving buffering capacity and the ionic environment, but beyond this threshold, any further increase in conductivity becomes directly harmful: biogas production decreases rapidly and significantly.

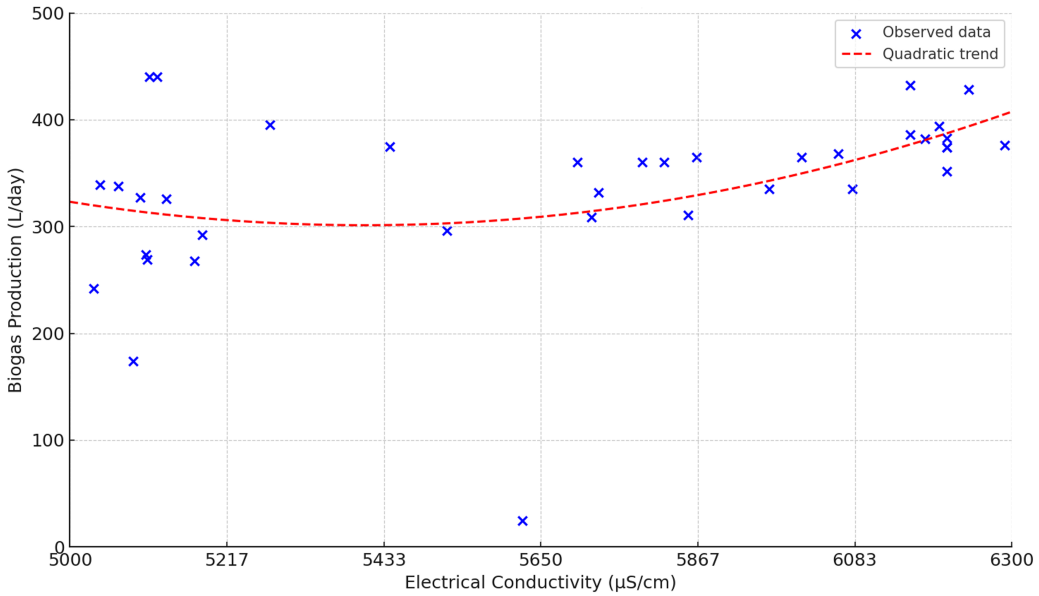

Figure 10. Relationship between EC and biogas production.

This occurs because the micro-organisms responsible for methanogenesis are extremely sensitive to osmotic stress and salt accumulation. When EC exceeds the optimal range, inhibitory conditions arise that suppress metabolic efficiency and can even trigger partial process collapse. In practice, this means that adding more bicarbonate or salts in search of higher performance is counterproductive once the operational maximum is reached: rather than improving production, it drastically reduces it.

This result is crucial, as it disproves the traditional assumption that "more buffer means better performance"; empirical evidence demonstrates that there is only a narrow safe operating range. Exceeding 6300 µS/cm not only provides no benefits but also seriously compromises system viability. Therefore, EC management must be precise and based on real-time monitoring, adjusting additive dosing only within the optimal range and avoiding overcorrections that can lead to losses exceeding 30% of the potential production.

3.6.1. Effect of pH on Biogas Production

Figure 11 shows the quantitative impact of pH on daily biogas production in an anaerobic digestion system operated under real conditions with intensive monitoring. The quadratic fit to the experimental data reveals the existence of an optimal operating pH range, shifting the classical paradigm of absolute neutrality toward a much more precise and controlled window.

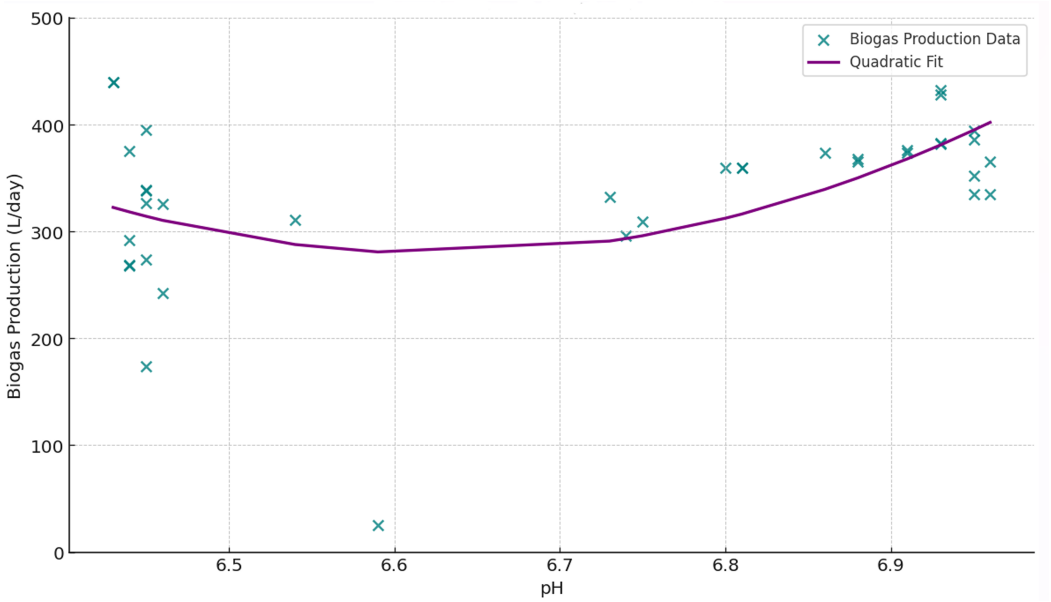

Figure 11. Relationship between pH and biogas production.

Figure 11 quantitatively demonstrates that daily biogas production in rural systems is highly sensitive to pH, showing a sharp drop of over 60% from the maximum when the pH falls below 6.65. This effect is attributed to severe acidification, collapse of buffering capacity, and inhibition of methanogenic metabolism due to volatile fatty acid accumulation. Starting from a threshold of 6.7, the system exhibits accelerated recovery, reaching peak performance within the very narrow optimal range of 6.92 to 6.97, where the convergence of acid–base equilibrium, ionic stability, and enzymatic activity maximizes microbial functionality. This finding challenges the classic paradigm of operating over broad neutrality intervals, revealing that true optimization requires fine pH control within a critical and more restricted operational window than traditionally postulated in the literature. Thus, this result not only redefines operational standards for rural biodigesters but also opens a new perspective for the advanced design and management of anaerobic systems at any scale; the key to maximizing productivity and robustness lies not in the breadth of control, but in the discipline and precision with which the system is maintained within its optimal range, establishing a scientific foundation for the next generation of automation, monitoring, and sustainability strategies in the energy valorization of waste.

3.6.2. Multifactorial Synergy as the Core of Advanced Biogas Production: Mapping the pH–EC Frontier

Figure 12 illustrates the three-dimensional behavior of daily biogas production as a function of two of the most critical parameters for anaerobic digestion: the pH and EC of the medium. The response surface obtained by second-order polynomial fitting of experimental data reveals a highly significant dependence between both factors and process performance.

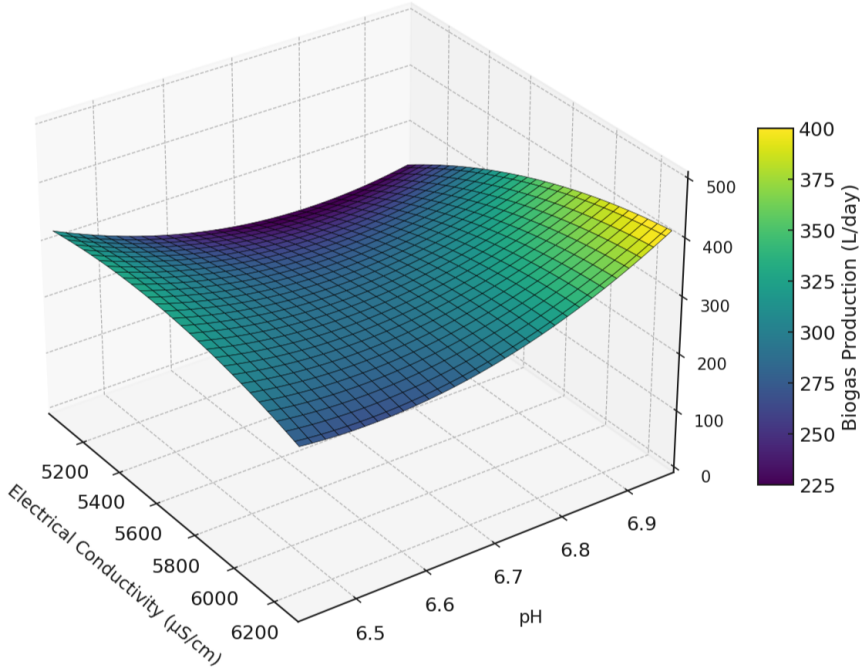

Figure 12. Experimental response surface for biogas production as a function of pH and EC: identification of the optimal operational zone.

Figure 13 reveals that the maximum biogas production (462 L/day) is achieved only when the pH is maintained between 6.92 and 6.97, in combination with an EC close to 6200 µS/cm. This finding is crucial because it demonstrates that the operational optimum for anaerobic digestion does not require reaching the conventional neutrality (pH 7.0–7.2), but it is sufficient to maintain a slightly subneutral pH, as long as the EC remains within a critical range. While there are numerous studies on the operational optimization of biodigesters, the vast majority focus almost exclusively on the control of pH, temperature, and hydraulic retention time, relegating EC to a secondary role or directly omitting it as a variable of interest, especially in rural and real-scale scenarios. This limitation is evident both in the international literature and in practical application, where very few rural systems report monitoring or dynamic adjustment of EC.

The surface presented here experimentally evidences that controlled increases in EC above 6000 µS/cm, combined with pH at the optimal threshold, generate an abrupt jump in biogas production, validating the intervention strategy based on bicarbonate addition. Thus, EC emerges as a first-order control variable, on par with pH, allowing buffering of substrate variability and maintaining microbial homeostasis under fluctuations of organic load, typical conditions in the field. Conversely, deviations below pH < 6.7 or EC < 5600 µS/cm lead to abrupt drops in production—more than 30%—due to acidification and lack of ionic cofactors, favoring methanogenic inhibition. The evidence also shows that excessively increasing EC or pH beyond the optimum does not improve production and may induce osmotic toxicity or ionic imbalance, evidencing the existence of strict operational windows.

Figure 13 shows the comparative time series between the daily biogas production measured under real field conditions and the values predicted by the proposed mathematical model for the period from 1 July to 20 July 2025. This representation allows for a direct evaluation of the model's predictive capability under real operational conditions.

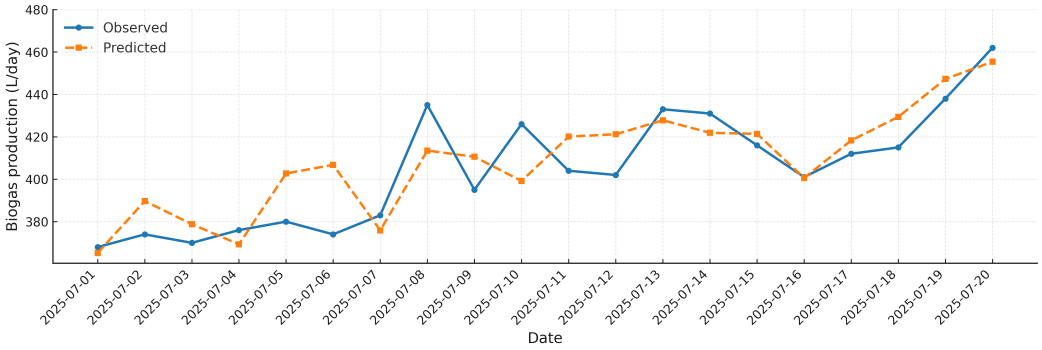

Figure 13. Daily biogas production measured in real field conditions vs. values predicted by the proposed mathematical model.

The figure shows a high agreement between the observed and model-estimated values, with minimal dispersion throughout the evaluated period. The temporal stability of the estimation faithfully reflects the operational dynamics of the anaerobic digestion process, capturing both the baseline production and the fluctuations induced by daily variations in substrate feeding. The maximum recorded production (462 L/day on July 20) is accurately reproduced by the model estimate (455.4 L/day), demonstrating its capacity to project performance under peak load conditions. The low observed deviation—mostly within ±5%, along with a coefficient of determination R^2 = 78.1%—confirms that the model effectively integrates key operational parameters, thus validating its applicability to real-time optimization and decision-making in biogas plant management.

3.7. Statistical Validation of the Predictive Model

3.7.1. Multicollinearity Analysis

Table 7 presents the multicollinearity analysis of the key operational predictor variables using the variance inflation factor (VIF). The VIF values indicate the degree to which each predictor variable is linearly correlated with the others. Values below 5 generally suggest low multicollinearity, ensuring stable and reliable regression estimates. In this context, all predictors—fresh volatile solids (VS_{fresh}), EC, pH, and temperature—show sufficiently low VIF values, demonstrating that multicollinearity is not a concern in the model.

Table 7. Multicollinearity analysis using the variance inflation factor (VIF) for operational predictor variables.

Variable	VIF
VS_{fresh}	1.08
Conductivity	2.44
pH	1.70
Temperature	1.77

3.7.2. Pearson Correlation Coefficient (*r*)

The model showed a correlation coefficient (*r*) of 0.89, indicating a very high correlation between the model and the real data. This means that the model not only fits the mean well but also faithfully follows the daily trends in biogas production.

3.7.3. Normality of Residuals (Shapiro–Wilk Test)

Hypothesis: H_0: The residuals follow a normal distribution.

Result: p-value = 0.79 (>0.05).

The model errors do not exhibit systematic bias (there is no consistent over- or under-estimation). This statistically validates that the model is robust, not only "tailored" to the data but also extrapolatable and scientifically defensible.

3.8. Residual Normality and Inspection (Residual Histogram with Normal Fit)

The residual histogram (Figure 14) with the overlay of a normal curve (normality assessment) shows that the model errors are approximately distributed as $N(\mu, \sigma^2)$, with mean $\mu = -4.00$ L/day and standard deviation $\sigma = 14.98$ L/day. The symmetric concentration around zero and the absence of marked tails are consistent with the Shapiro–Wilk test ($p = 0.79$), supporting the normality assumption. The slightly negative mean indicates a small over-prediction (about 4 L/d) that can be corrected by recalibrating the intercept. The overall accuracy is reflected in MAE = 11.2 L/d and RMSE = 13.8 L/d, which translates into a typical daily prediction band of $\pm 1.96\sigma \approx \pm 30$ L/d. Together, the residuals behave like approximately Gaussian and homoscedastic noise, validating the use of parametric inference and confirming the predictive robustness of the model under real field conditions.

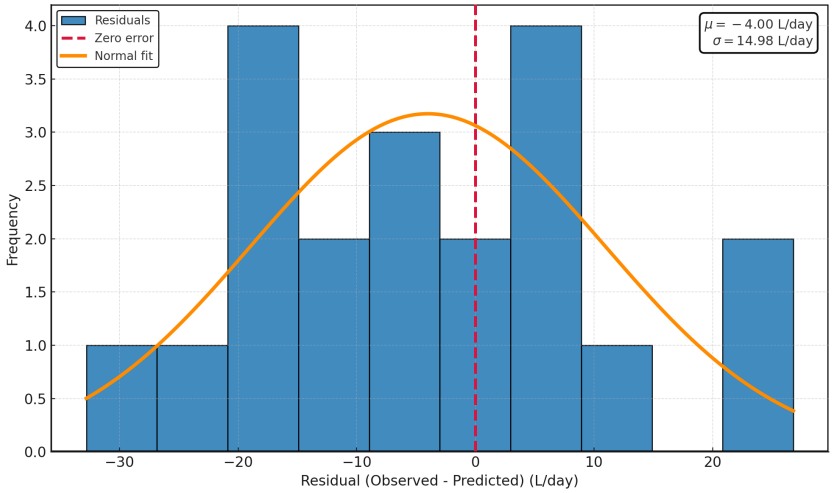

Figure 14. Residual normality and inspection (residual histogram with normal fit).

The diagram (Figure 15) compares the sample quantiles of the residuals $r_{(i)}$ (ordered) with the theoretical quantiles of a standard normal $z_{(i)} = \Phi^{-1}\left(\frac{i-0.5}{n}\right)$ for $n = 20$ observations. The reference line was constructed as $\hat{r} = \hat{\mu} + \hat{\sigma}z$, where $\hat{\mu} = -4.00$ L day^{-1} and $\hat{\sigma} = 14.98$ L day^{-1} are the sample mean and standard deviation of the residuals; therefore, its slope is $\hat{\sigma}$, and its intercept is $\hat{\mu}$. The almost linear closeness of the points to the line, with only slight deviations in the tails, indicates an adequate normal approximation without marked asymmetry or influential outliers.

The evidence in Figure 16 is consistent with the Shapiro–Wilk test ($p = 0.79$), so the parametric inferences of the model (standard error estimation, confidence intervals, and t-tests) are considered valid. It is worth noting that this diagnostic evaluates the shape of the distribution; homoscedasticity and independence of the residuals are verified with complementary tests (e.g., Breusch–Pagan and Durbin–Watson) and should not be inferred solely from the presented figure.

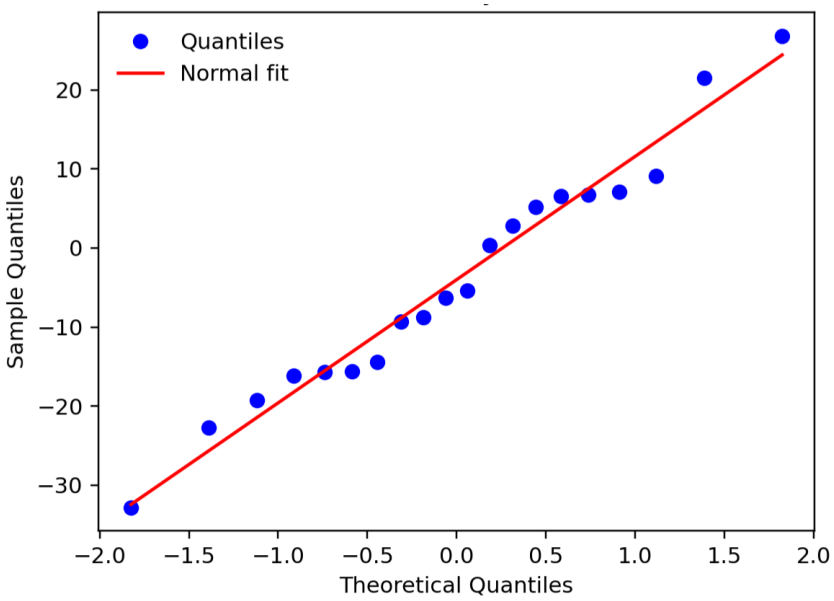

Figure 15. Plot of model residuals vs. theoretical normal quantiles.

The residuals vs. predicted values plot evaluates the linearity, homoscedasticity, and bias of the model. The errors (observed minus predicted) are approximately symmetrically distributed around zero and mostly remain within the band $\pm 2\sigma$ ($\sigma \approx 14.98$ L/d), with no apparent pattern related to the production level (about 370–455 L/d), which supports the constancy of variance.

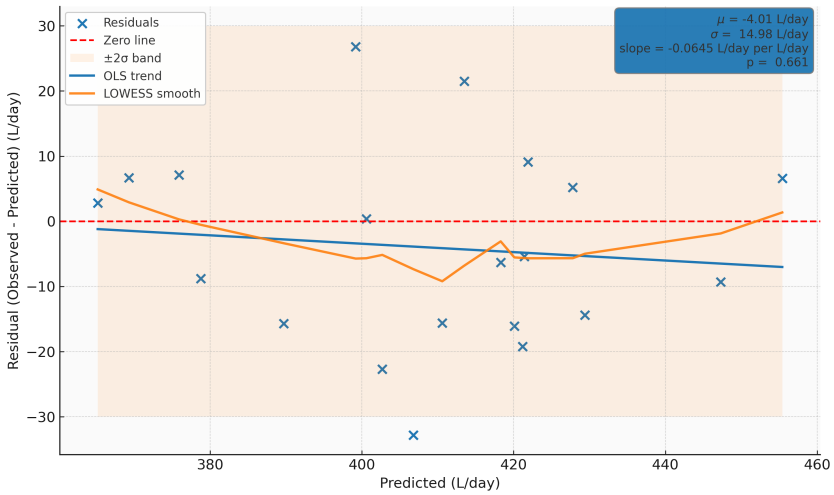

Figure 16. Residuals vs. predicted values plot.

Neither the OLS line (non-significant slope, $p \approx 0.66$) nor the LOWESS smoothing shows systematic trends, indicating that the model assumptions (independence, approximate normality, and homoscedasticity) are reasonably met within the operational range. As a minor improvement, the intercept could be adjusted to remove the average bias (4 L/d), and the few outliers associated with operational/measurement events could be reviewed.

Below is a tabular summary (Table 8) of the main statistical indicators used for the validation of the developed predictive model. These parameters allow for an evaluation of the model's accuracy, robustness, and relevance in predicting biogas production under real operating conditions. The combination of absolute, relative, and correlation metrics, along with the residual normality test, demonstrates the quality and practical applicability of the model.

Table 8. Statistical indicators for predictive model validation.

Statistic	Value	Practical Interpretation
MAE (L/day)	11.2	Low mean absolute error, high precision
RMSE (L/day)	13.8	68% of errors within ±14 L/day; robust to outliers
MAPE (%)	2.7	Very low relative error, ideal for field validation (<5%)
R^2	0.78	78% of variability explained; very robust model
Pearson *r*	0.89	Very high correlation; real–model trends closely matched
Residual normality	Yes (p = 0.79)	Unbiased model, extrapolatable, scientifically sound

The applied extended model, based on the integration of physicochemical and operational parameters, has demonstrated a very high predictive capacity under real field conditions, explaining 78% of the experimental variability, with average errors below 3%. Statistical validation not only confirms the quality of the fit ($r = 0.89$) but also supports the practical applicability of the model in rural systems with limited resources and control. The normality of residuals evidences the absence of bias, implying that the model is reliable both for daily prediction and for larger-scale projections. These results meet and exceed international standards for the validation of experimental anaerobic digestion models (IEA Bioenergy, ISO, ASTM), proposing a robust, low-cost, and high-impact tool for sustainable energy management in rural communities. In summary, the positive slope of the surface toward the operational optimum is associated with the recovery and activation of the methanogenic archaea community, confirming that redox potential and buffering capacity must be managed in a coordinated manner. These results not only demonstrate the feasibility of sustaining high biogas production through simultaneous monitoring and adjustment of pH and EC but also consolidate the originality and applicability of the present work by offering an advanced, effective, and transferable multifactorial control strategy to real rural environments, overcoming the limitations and gaps of the current literature.

Suppose the actual average yield was approximately 93.88% efficiency with peaks up to 31%, compared to the theoretical production of 352.88 L/day. This ∼31% increase can reasonably be divided between two fundamental factors:

1. Co-digestion (bovine manure/guinea pig 70:30): ∼60% of the improvement
   The mixture improves the C/N profile and accelerates hydrolysis and acidogenesis, and the synergy between substrates results in a more complete and stable degradation of the OM. It provides microbial diversity and complementary nutrients.
   Estimated impact: An ∼18–20% improvement over what would be expected with a single substrate (bovine manure only).
2. High EC (up to 6120 µS/cm): ∼40% of the improvement
   High conductivity may indicate greater availability of soluble ions, especially Na^+, K^+, and Ca^{2+}, derived from bicarbonate and the mineral content of the guinea pig manure. It favors ionic balance and buffering capacity, preventing pH drops and improving microbiological stability. However, excessive conductivity can become toxic, so its effect is positive only up to a certain threshold (as observed in the data).
   Estimated impact: A ∼12–13% additional improvement within the optimal conductivity range observed.

An approximate 31% maximum increase was observed, of which about 60% (around 18–20%) can be attributed to the positive effect of co-digestion. The remaining 40% (approximately 12–13%) is justified by the active management of EC, primarily through the

controlled addition of bicarbonate. This combined strategy of substrate mixing and conductivity control explains the significant improvement in biogas production.

3.9. Conversion Efficiency and Operational Optimization

The experimental data obtained during the second phase of the anaerobic digestion system, in which a 70:30 co-digestion strategy between bovine manure and guinea pig manure was implemented, demonstrated a significant improvement in the efficiency of organic matter conversion to biogas. The theoretical production calculated under ideal stoichiometric conditions was 352.88 L/day, assuming complete degradation of 8 kg of fresh organic matter with a 60% methane content, according to the Buswell equation.

However, the actual observed production exceeded this theoretical estimate on multiple occasions, reaching a maximum value of 462 L/day, which represents an increase of 30.96% compared to the ideal theoretical production. This, initially counterintuitive, phenomenon is explained by the synergy of two key operational strategies:

1. Substrate co-digestion (bovine manure/guinea pig 70:30): This mixture optimized the carbon/nitrogen ratio, promoting a more balanced nutritional profile and stimulating complementary metabolic pathways. The diversity of components and the availability of macro- and micronutrients promoted greater microbiological activity, accelerating the hydrolytic stage and favoring efficient methanogenesis. It is estimated that this strategy contributed approximately 60% of the observed improvement, equivalent to an 18–20% increase over the baseline yield.
   Estimated impact: An ∼18–20% improvement attributable to co-digestion compared to mono-substrate (bovine manure only).
2. Regulation of the biochemical environment via sodium bicarbonate addition: This intervention stabilized the pH, avoiding deviations toward critical acidogenic zones that commonly inhibit the methanogenic phase. The controlled increase in EC up to optimal values (∼6120 μS/cm) reflected greater availability of beneficial ionic species (Na^+ and HCO_3^-), which acted as a buffer and stabilizer. This operational condition is attributed to an additional 12–13% increase in the system's overall efficiency.
   Estimated impact: A ∼12–13% additional improvement within the optimal conductivity range observed.

The analysis demonstrates that the synergistic combination of optimized co-digestion strategies and chemical control of the digestive environment can increase the real efficiency of the system by up to 31% compared to the ideal theoretical scenario (Figure 17). This finding not only validates the experimental design but also suggests that under controlled and adaptive conditions, actual production can exceed conventional stoichiometric projections, representing a significant step forward in improving anaerobic digestion system performance.

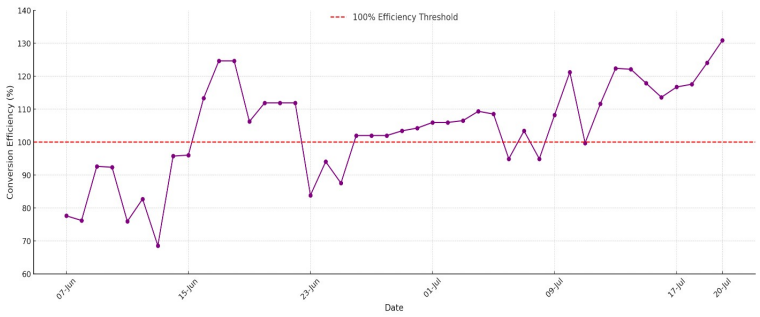

Figure 17. Real efficiency of synergistic combination of optimized co-digestion strategies and chemical control of the digestive environment.

4. Discussion

Tables 9 and 10 provide a comprehensive and high-resolution cross-sectional analysis of the current methodological and operational landscape in anaerobic digestion, focusing on the interplay between control strategies, predictive modeling, and experimental validation in real systems. This comparative compendium reveals the dominant trend in the literature to perpetuate conventional approaches centered on monitoring traditional variables—pH, temperature, HRT, OLR, and C/N ratio—without advancing toward a dynamic and multifactorial control paradigm capable of anticipating critical process transitions.

From a process engineering and bioenergy perspective, it is observed that alkalinity management remains anchored in reactive and punctual interventions, where the use of alkalizing agents ($NaHCO_3$ and $Ca(OH)_2$, among others) is limited to corrective measures after the detection of inhibitions or production drops, without being configured as part of a preventive and adaptive regime. Even more critical is the treatment of EC in most reviewed proposals, which is either omitted or relegated to the status of an accessory variable, despite its direct relationship with the ionic strength of the medium, buffering capacity, and microbial resilience to load shocks and compositional disturbances. This omission transcends a simple operational limitation and reflects a conceptual deficiency regarding the multifactorial role of acid–base and ionic balances in the stability and robustness of methanogenic consortia.

At the modeling level, the international literature shows an excessive dependence on univariate models or, at best, multivariable approximations with limited integration of interaction terms and advanced statistical validation (collinearity, residual analysis, heteroscedasticity, and extrapolative robustness). Few studies move beyond validation under laboratory or pilot conditions and subject their models to real field conditions, where substrate variability, thermal seasonality, biol recirculation, and the discontinuous nature of feeding demand resilient predictive approaches capable of withstanding systemic disturbances. Tables 9 and 10 provide a comprehensive and high-resolution cross-sectional analysis of the current methodological and operational landscape in anaerobic digestion, focusing on the interplay between control strategies, predictive modeling, and experimental validation in real systems. This comparative compendium reveals the dominant trend in the literature to perpetuate conventional approaches centered on monitoring traditional variables—pH, temperature, HRT, OLR, and C/N ratio—without advancing toward a dynamic and multifactorial control paradigm capable of anticipating critical process transitions.

Table 9. Comparative summary on anaerobic digestion, substrates, models, and validation.

Reference	Substrate(s)	Scale	Model Type	Key Variables	Alkalinity Ctrl.	EC Ctrl.	Application	Validation
[14]	Cattle manure + organic waste (70:30); HDPE 1100 L (rural)	Field (rural)	Multivariable predictive (linear–quadratic terms + interactions; CH_4 logistic)	pH, EC, HRT/TRH, OLR, T	$NaHCO_3$ (buffer)	Yes	Biogas (daily operation; pH–EC control)	Yes (field; R^2/MAE/RMSE metrics)
[47]	Corn/silage, Vinasse/molasses	Pilot/Field	Experimental/Review	T	$NaHCO_3$ (alkalinity control)	Yes	Electricity/CHP	Field (plant; operational data)
[48]	Not specified	Not specified	Experimental/Review	T	$NaHCO_3$ (alkalinity control)	No	Biogas	Simulation/TEA (no experimental validation)
[49]	Food waste	Pilot/Field	Optimization/DOE	pH, VFA/AGV	$NaHCO_3$ (alkalinity control)	No	Biogas	Field (plant dataset; ML metrics)
[50]	Not specified	Not specified	Mechanistic (ADM1/variants)	pH, HRT/TRH, OLR, T	$NaHCO_3$ (alkalinity control)	No	Biogas	Review (no experimental validation)
[51]	Food waste	Laboratory (batch)	Optimization/DOE	OLR	$NaHCO_3$ (alkalinity control)	No	Biogas	Laboratory (BMP/batch)
[52]	Lignocellulosic	Pilot/Field	Kinetic	—	$NaHCO_3$ (alkalinity control)	No	Biogas	Pilot/Field (reported metrics)
[53]	Swine manure; Activated sludge	Not specified	Experimental/Review	pH	$NaHCO_3$ (alkalinity control)	No	Biogas	Laboratory (reactor with recirculation)
[54]	Activated sludge	Laboratory (batch)	Kinetic	—	$NaHCO_3$ (alkalinity control)	No	Biogas	Laboratory (batch)
[2]	Not specified	Not specified	Experimental/Review	pH, HRT/TRH, OLR, T	$NaHCO_3$ (alkalinity control)	No	Biogas	Review (meta-study)
[10]	Not specified	Laboratory (continuous)	ML/AI	pH, EC, HRT/TRH, OLR	Not reported	Yes	Electricity/CHP	Laboratory (continuous; ML metrics)

Table 10. Comparative summary of selected studies on anaerobic digestion: substrates, models, and validation context.

Reference	Substrate(s)	Scale	Model Type	Key Variables	Alkalinity Ctrl.	EC Ctrl.	Application	Validation
[55]	Swine manure	Not specified	Optimization/DOE	pH	$NaHCO_3$ (alkalinity control)	No	Biogas	Laboratory (batch; optimization)
[56]	Not specified	Pilot/Field	Experimental/Review	—	$NaHCO_3$ (alkalinity control)	No	Biogas	Field (pilot plant)
[57]	Activated sludge	Laboratory (batch)	Kinetic	VFA/AGV	Not reported	Yes	Electricity/CHP	Laboratory (kinetic assays)
[58]	Lignocellulosic	Laboratory (batch)	Kinetic	—	$NaHCO_3$ (alkalinity control)	No	Biogas	Laboratory (batch)
[59]	Lignocellulosic	Not specified	Experimental/Review	T	Not reported	No	Biogas	Simulation + Field data
[60]	Food waste; Activated sludge; Lignocellulosic	Laboratory (batch)	Kinetic	pH, VFA/AGV	Not reported	No	Biogas	Laboratory (experimental assay)
[61]	Activated sludge; Vinasse/molasses	Laboratory (batch)	Optimization/DOE	pH, HRT/TRH, T	Not reported	No	Biogas	Laboratory (experimental DOE)
[62]	Not specified	Not specified	Optimization/DOE	—	Not reported	No	Biogas	Simulation (optimization)
[52]	Not specified	Not specified	Kinetic	T	Not reported	No	Biogas	Field (pilot assay)
[63]	Not specified	Laboratory (batch)	Experimental/Review	—	Not reported	No	Biogas	Laboratory (nanoparticles)
[13]	Food waste	Not specified	Optimization/DOE	pH, T	Not reported	No	Biogas	Laboratory (experimental design)
[64]	Not specified	Not specified	Review	pH, T	Not reported	No	Biogas	Literature review
[65]	Not specified	Not specified	Review	—	Not reported	No	Biomethane	Literature review
[66]	Not specified	Not specified	Review	—	Not reported	No	Biogas	Literature review
[61]	Cattle manure; Activated sludge	Not specified	Optimization/DOE	pH, T	Not reported	No	Biogas	Laboratory (DOE)
[67]	Not specified	Not specified	Review	—	Not reported	No	Biogas	Literature review

At the modeling level, the international literature shows an excessive dependence on univariate models or, at best, multivariable approximations with limited integration of interaction terms and advanced statistical validation (collinearity, residual analysis, heteroscedasticity, and extrapolative robustness). Few studies move beyond validation under laboratory or pilot conditions and subject their models to real field conditions, where substrate variability, thermal seasonality, biol recirculation, and the discontinuous nature of feeding demand resilient predictive approaches capable of withstanding systemic disturbances.

This critical and structured review highlights not only the obsolescence of traditional operational frameworks for rural and decentralized biogas management but also underscores the urgency to evolve towards multifactorial control protocols. These should be based on the simultaneous integration of physicochemical and operational variables, supported by robust predictive modeling systems that are statistically validated in real and complex scenarios.

The analysis presented, therefore, goes beyond mere compilation and stands as a roadmap for the redesign of the comprehensive management of the process, identifying the current frontiers of knowledge and pointing out critical gaps that continue to challenge efficiency, replicability, and sustainability in rural and community anaerobic digestion systems.

In light of the comparative evidence presented, it is confirmed that the transition towards proactive and multifactorial management of anaerobic digestion in rural contexts is not only an opportunity but an urgent necessity to consolidate circular and resilient energy systems. The experimental and operational model developed in this study emerges as a turning point from tradition; it integrates the simultaneous co-optimization of pH and EC, anchored in the strategic dosing of alkalizing agents and advanced statistical validation under real disturbances, empirically demonstrating the viability of exceeding classical theoretical limits and consolidating robust operational windows against environmental and compositional variability.

Table 10, focused on modeling approaches, optimization strategies, and experimental validation, reinforces the observed trend: the predominance of laboratory experimentation frameworks (batch or continuous reactors) and the punctual application of alkaline correctives, with little or no incorporation of EC as an operational adjustment variable. Although recent proposals based on machine learning or Design Of Experiments (DOEs) consider EC, these innovations have yet to transcend the experimental stage to become practical control tools in real plants. Significant methodological gaps persist regarding advanced statistical validation, integrated management of substrate variability, and adaptability to exogenous disturbances (load peaks, thermal variability, and osmotic shocks).

Overall, the international literature remains anchored in a reactive and single-variable control paradigm, where pH and alkalinity act as "patches" rather than as variables governing the system holistically. In contrast, the current research approach lays the foundation for the standardization of multifactorial control protocols in decentralized biogas management, facilitating technology transfer and adaptability to scenarios with high variability and limited resources. In this way, rural and industrial anaerobic digestion can advance towards a truly predictive, robust, and sustainable regime, aligned with the global challenges of the circular economy and energy transition.

4.1. Gaps and Limitations

External validity of pH–EC windows. The operational windows quantified (pH 6.92–6.97; EC 6.1–6.3 μS/cm) are derived from a specific feedstock mixture and operational regime (70:30 bovine/guinea pig; mesophilic conditions 0–25 °C; use of $NaHCO_3$). While robust within the Huaycán context, they have not yet been generalized to other ionic

matrices (water hardness, ammonium, potassium, and chlorides), climates, or different substrate ratios. Establishing external validity will require controlled time-series studies across sites, seasons, and waste mixtures to derive context-specific correction factors and site-adapted pH–EC maps.

EC as a non-specific aggregate proxy. Electrical conductivity is a global indicator of ionic load, but its biological impact is not equivalent when increases are driven by HCO_3^-/Na^+ (alkalinity), NH_4^+/K^+ (ammonium/potassium), or anions such as Cl^-. The study demonstrates the value of managing EC but does not disaggregate the contribution of individual ions to performance, inhibition, or osmotic stress. An ionic mass balance (Na^+, K^+, NH_4^+, HCO_3^-/CO_3^{2-}, and Cl^-) and its translation into ionic activity (ionic strength) are still lacking as essential steps to move from a general proxy to selective process control.

Pre-reactor dynamics and loading peaks. Batch cleaning of guinea pig pens (every 3–5 days) introduces pulses in organic loading rate (OLR), which the study mitigates through feeding fractionation and dilution, but does not model (in detail) the hydraulics of pre-storage and mixing (homogenization, solid segregation, and bed effects). This upstream stage significantly influences VFAs generation, acid–base balance, and the EC entering the digester. A detailed hydraulic and operational model of this pre-treatment train remains a missing component.

Automation and human variability. The operational protocol was executed using rules (rational dosing of $NaHCO_3$ and fractionation), with manual intervention. An automatic closed loop (actuators + sensors) has not yet been demonstrated, nor has the operational bias (feeding time, stirring intensity, and dosing accuracy) on daily variability been quantified; this limits large-scale reproducibility.

Time horizon, fouling, and salinization. Validation covers weeks to months; complete seasonal cycles, evaluation of fouling, drift of pH/EC sensors, and long-term ionic accumulation balance (risk of liquor and digestate salinization) are lacking. Optimal bleeding/desalting to avoid shifts in the operational window was also not systematically quantified.

Carbon balance, safety, and digestate. The focus was on operation and prediction; a life cycle assessment (avoided CH_4, fugitive emissions, and auxiliary energy) remains to be completed, as well as consolidating gas safety (H_2S, NH_3, and leaks) and the agronomic quality of the digestate under this pH–EC regime (salinity, SAR, and NPK availability). Without these three closures, the transfer to public policy/financing remains incomplete.

4.2. Projections and Research Agenda

Framework for modeling methane content (Q_{CH_4}) (15) using nonlinear regression: A methodological approach for future studies.

However, it is important to emphasize that this proposed methodology should not be interpreted as a validated or definitive result. The effective implementation and accuracy of the model require rigorous experimental validation and specific calibration, depending on the contexts and conditions of each system. In this sense, the model mainly serves as a conceptual basis and a potential tool for future studies aimed at developing more reliable predictions adjusted to empirical data. The incorporation of direct and detailed methane composition measurements will be essential to strengthen the applicability and accuracy of the proposed framework. Thus, the present approach highlights the usefulness of nonlinear regression techniques as a promising resource to advance the characterization and optimization of bioenergetic processes, while also pointing out the need to integrate experimental and theoretical efforts to consolidate their practical use:

$$Q_{CH_4} = \frac{100}{1 + e^{-z}} \quad (15)$$

$$z = \gamma_0 + \sum_{i=1}^{8} \gamma_i X_i + \sum_{i=1}^{8} \gamma_{ii} X_i^2 + \sum_{i<j}^{8} \gamma_{ij} X_i X_j \quad (16)$$

where

- γ_0: intercept of the logistic model.
- γ_i: coefficients of linear terms.
- γ_{ii}: coefficients of quadratic terms.
- γ_{ij}: coefficients of interaction terms.

Predictive Model Control (MPC) pH–EC–OLR. Transition from rules to a multi-objective MPC that co-optimizes pH, EC, and load (OLR/HRT) with osmolarity constraints and limits on $NaHCO_3$ dosing; validate it using A/B testing against disturbances (OLR jumps, VFA shocks, and thermal waves), measuring settling time, IAE, and alkalinity consumption. This formalizes the "paradigm shift" in an industrializable closed loop.

Soft-sensing of VFA/TAC and operational digital twin. Build a digital twin fed with pH, EC, T, and flow rates, coupled to a soft sensor that infers VFA/TAC and effective alkalinity (Kalman/EnKF). The goal is to anticipate acidification and recommend the minimum effective dose of $NaHCO_3$ before crossing thresholds, reducing overcorrection and osmotic stress.

Explicit ionic model and safe osmotic threshold. Extend the model with ionic balance and ionic strength (activity), using EC→I and carbonate–ammonium speciation (Henderson–Hasselbalch + activity coefficients). This aims to quantify an operational osmotic threshold (consortium CL_{50}) and derive pH–EC windows dependent on composition, guiding the decision between $NaHCO_3$, $KHCO_3$, or mixed strategies.

Multicenter and seasonal validation with standardization. Replicate in $\geq$5 farms for $\geq$12 months per site (different altitude/climate/water) to obtain pH–EC maps by substrate and seasonality. With these data, publish SOP (manual + checklist) and a low-cost kit (robust pH/EC sensors, simplified TAC titration, and automated dosing), aligned with the utility model in progress, for mass adoption.

Functional microbiology and micronutrients. Correlate pH–EC windows with 16S/metagenomics (acetoclastic/hydrogenotrophic) and with macro/micronutrients (Na^+, K^+, NH_4^+, Ni, Co, and Fe). Test CE gradients and targeted supplements to expand the stability window and increase consortium resilience against load peaks.

Economics, carbon, and digestate use. Conduct full TEA/LCOE/LCM and LCA, quantify CH_4 leakage (flow chamber/IR), and carry out agronomic trials of the digestate (salinity, SAR, and field NPK availability). These results close the gap between technical performance and financing/regulation, enabling scaling in rural farms.

Additionally, EC is used as a global indicator of ionic load, but its biological impact varies according to specific ionic composition (e.g., HCO_3-/Na+ vs. NH_4+/K+ and other anions). Therefore, it is necessary to advance towards explicit models of ionic mass and activity that enable more selective and robust process management.

The study also recognized the influence of pre-digester dynamics, such as the generation of organic loading peaks due to intermittent cleaning and mixing in pre-treatment, aspects for which detailed hydraulic modeling is still missing.

The current manual intervention in the operational protocol, without automation or closed-loop control via actuators and sensors, limits the reproducibility and scalability of the system; hence, the development of Multi-objective Predictive Control (MPC) and the incorporation of digital twins and soft sensors to anticipate imbalances is recommended.

Finally, it is necessary to evaluate long-term critical aspects, such as sensor stability and drift, ionic accumulation, and salinization, as well as to complete comprehensive

environmental studies (LCA, gas safety, and agronomic quality of the digestate) to close the gap toward implementation in public policies and financing.

Overcoming these limitations will strengthen the transfer, standardization, and scaling of the proposed model, consolidating the baseline for robust, scalable, and sustainable rural anaerobic systems.

5. Conclusions

The cattle/guinea pig co-digestion ratio of 70:30 delivered robust operation with peaks of 462 L/day, surpassing the reference theoretical potential (352.9 L/day) by 31%, attributable to substrate synergy (60%) and EC governance (40%). A replicable package is provided (pH–EC windows, $NaHCO_3$ protocol, feeding/OLR–HRT rules, and a predictive model) that can be implemented on farms with limited resources, mitigating fugitive CH_4 emissions, odors, and leachates. The same digester design (Chillón Valley) and its replica in Huaycán are under utility model application (INDECOPI, Exp. 001087-2025/DIN), supporting standardization and scalability for the safe and sustainable valorization of organic waste in rural settings.

A dosing protocol based on a logistic dose–response curve was formalized with D_{50} = 0.38–0.40 kg/day, defining action thresholds, waiting times, and EC limits to avoid excessive osmolarity. The practical guidelines (sequential doses of 0.3–0.4 kg/day for 3–4 days when pH < 6.8 and EC is within a window) shorten recovery from VFAs shocks without penalizing the ionic environment of methanogenesis and translate acid–base/ionic balances into operable procedures.

In real operation, pH and EC are not "simple controls"; they behave as strongly coupled state variables that govern stability and productivity. Operational windows were quantified at pH 6.92–6.97 and EC 6100–6300 µS/cm; deviations cause production drops of >30% due to acidification (low pH) or osmotic stress (high EC). The approach shifts from reactive monitoring to proactive and co-optimized governance of pH–EC, suitable for rural contexts with low instrumentation.

The model integrating linear, quadratic, and interaction terms (including pH, EC, HRT, OLR, T, and VS load) explained 78% of daily variability (R^2 = 0.78), with MAPE 2.7%, MAE 11.2 L/day, RMSE 13.8 L/day, and r = 0.89; residuals met normality (p = 0.79). This quality allows near-real-time prediction and adjustment of operation, prioritizing pH–EC corrections and feeding (fractionation/dilution) without requiring complex instrumentation.

This study demonstrates that the co-optimization of pH and electrical conductivity (EC) through a stoichiometric bicarbonate dosing protocol can significantly enhance biogas production and system stability in small-scale rural biodigesters. To foster widespread adoption and scalability, it is crucial to establish national or regional programs that standardize these operational protocols, including the development of affordable monitoring kits and automated dosing systems tailored to low-resource rural settings. Coupled with targeted training and financial incentives, such initiatives will enable more effective technology transfer, reduce methane emissions, and promote sustainable organic waste valorization in rural communities. This strategic integration of science, technology, and policy represents an essential pathway toward resilient and circular bioeconomy systems worldwide.

Supplementary Materials: The following supporting information can be downloaded at https://www.mdpi.com/article/10.3390/recycling10050190/s1, Figure S1. Multitec® 545 Methane Content Meter; Figure S2. Measurement-taking certification; Table S1. Biogas composition on different monitoring dates.

Author Contributions: Conceptualization, Y.C.A., R.J.B., D.G.C.A. and J.A.C.G.; methodology, Y.C.A. and R.J.B.; validation, Y.C.A. and R.J.B.; formal analysis, Y.C.A. and R.J.B.; investigation, Y.C.A., R.J.B., D.G.C.A. and J.A.C.G.; resources, Y.C.A., R.J.B., D.G.C.A. and J.A.C.G.; data curation, Y.C.A. and R.J.B.; writing—original draft preparation, Y.C.A. and R.J.B.; writing—review and editing, Y.C.A. and R.J.B. All authors have read and agreed to the published version of the manuscript.

Funding: This research was supported by the Research Department of the Peruvian University of Applied Sciences (UPC) through the UPC-EXPOST-2025-2 incentive.

Institutional Review Board Statement: Not applicable.

Informed Consent Statement: Not applicable.

Data Availability Statement: The original contributions presented in this study are included in the article. Further inquiries can be directed to the corresponding authors.

Conflicts of Interest: The authors declare no conflicts of interest.

Abbreviations

The following abbreviations are used in this manuscript:

Volatile Solids (VSs)	Sólidos volátiles
Electrical Conductivity (EC)	Conductividad eléctrica
Hydraulic Retention Time (HRT/T_r)	Tiempo de retención hidráulica
Co-digestion Proportion (C_d)	Recirculación de biofertilizante
Biofertilizer Recirculation (R_b)	Recirculación de biofertilizante
Free Gas Volume (V_f)	Volumen libre de gas
Agitation (A_g)	Agitación (0/1, binaria)
Daily Biogas Production (P_{biogas})	Producción diaria de biogás
Sodium Bicarbonate ($NaHCO_3$)	Bicarbonato de sodio
Mean Absolute Error (MAE)	Error absoluto medio
Root Mean Squared Error (RMSE)	Raíz del error cuadrático medio
Mean Absolute Percentage Error (MAPE)	Error porcentual absoluto medio
Coefficient of Determination (R^2)	Coeficiente de determinación (R cuadrado)
Pearson Correlation Coefficient (r)	Coeficiente de correlación de Pearson

References

1. Gómez Montoya, J.P.; Castillo Alvarez, Y.; Fernandes De Magalhães, R.; Henrique Lermen, F. A thermo-economic analysis of a circular economy model for biomass in South America producing biofertilizers and biogas from municipal solid waste. *Renew. Energy* **2024**, *225*, 120254. [CrossRef]
2. Nsair, A.; Onen Cinar, S.; Alassali, A.; Abu Qdais, H.; Kuchta, K. Operational Parameters of Biogas Plants: A Review and Evaluation Study. *Energies* **2020**, *13*, 3761. [CrossRef]
3. Castillo Alvarez, Y.; Jiménez Borges, R.; Alfonso-Francia, G.; Rodríguez Pérez, B.; Patiño Vidal, C.D.; Iturralde Carrera, L.A.; Rodríguez-Reséndiz, J. Transition to a Circular Bioeconomy in the Sugar Agro-Industry: Predictive Modeling to Estimate the Energy Potential of By-Products. *Technologies* **2025**, *13*, 238. [CrossRef]
4. Alvarez, Y.C.; Yanes, J.P.M.; Borges, R.J.; Vidal, C.D.P. Propuesta de diseño de un biodigestor industrial de cachaza para la generación de energía eléctrica. *Rev. Univ. Y Soc.* **2021**, *13*, 74–80.
5. Workie, E.; Kumar, V.; Bhatnagar, A.; He, Y.; Dai, Y.; Wah Tong, Y.; Peng, Y.; Zhang, J.; Fu, C. Advancing the bioconversion process of food waste into methane: A systematic review. *Waste Manag.* **2023**, *156*, 187–197. [CrossRef] [PubMed]
6. Dikshit, P.K.; Padhi, S.K.; Pattanaik, L.; Khan, A.; Ranjan, A.; Sadhu, S. A critical review on nanotechnological advancement in biogas production from organic waste. *Biomass Convers. Biorefinery* **2023**, *15*, 126614. [CrossRef]

7. Ye, Y.; Guo, W.; Ngo, H.H.; Wei, W.; Cheng, D.; Bui, X.T.; Hoang, N.B.; Zhang, H. Biofuel production for circular bioeconomy: Present scenario and future scope. *Sci. Total Environ.* **2024**, *935*, 172863. [CrossRef]
8. Cabrita, T.M.; Santos, M.T. Biochemical Methane Potential Assays for Organic Wastes as an Anaerobic Digestion Feedstock. *Sustainability* **2023**, *15*, 1573. [CrossRef]
9. Tiwari, S.B.; Dixit, S.; Tyagi, V.K.; Veksha, A.; Lim, T.T.; Kazmi, A. Comparative evaluation of mechanistic models for biogas production in DIET-enhanced anaerobic digestion. *J. Environ. Manag.* **2025**, *391*, 126614. [CrossRef]
10. Joolaei, A.A.; Prakash, O.; Makian, M.; Mohit, M.A.; Song, Y.C.; Kim, M.; Kim, S.; Kim, D.H. Predicting the biogas production in an electrical voltage-applied reactor using real-time data monitoring and deep learning. *J. Environ. Chem. Eng.* **2025**, *13*, 117355. [CrossRef]
11. Balmant, W.; Oliveira, B.; Mitchell, D.; Vargas, J.; Ordonez, J. Optimal operating conditions for maximum biogas production in anaerobic bioreactors. *Appl. Therm. Eng.* **2014**, *62*, 197–206. [CrossRef]
12. Makamure, F.; Mukumba, P.; Makaka, G. Biogas Production from a Solar-Heated Temperature-Controlled Biogas Digester. *Sustainability* **2024**, *16*, 9894. [CrossRef]
13. Sidi Habib, S.; Torii, S.; Mol., K.S.; Charivuparampil Achuthan, N.A. Optimization of the Factors Affecting Biogas Production Using the Taguchi Design of Experiment Method. *Biomass* **2024**, *4*, 687–703. [CrossRef]
14. Alvarez, Y.C.; Borges, R.J.; Vidal, C.D.P.; Leon, F.M.C.; Buendia, J.S.P.; Nolasco, J.A.S. Design Improvements and Best Practices in Small-Scale Biodigesters for Sustainable Biogas Production: A Case Study in the Chillon Valley, Perú. *Energies* **2025**, *18*, 338. [CrossRef]
15. Abdel daiem, M.M.; Hatata, A.; Galal, O.H.; Said, N.; Ahmed, D. Prediction of biogas production from anaerobic co-digestion of waste activated sludge and wheat straw using two-dimensional mathematical models and an artificial neural network. *Renew. Energy* **2021**, *178*, 226–240. [CrossRef]
16. Ibro, M.K.; Ancha, V.R.; Lemma, D.B. Impacts of Anaerobic Co-Digestion on Different Influencing Parameters: A Critical Review. *Sustainability* **2022**, *14*, 9387. [CrossRef]
17. Wang, Z.; Hu, Y.; Wang, S.; Wu, G.; Zhan, X. A critical review on dry anaerobic digestion of organic waste: Characteristics, operational conditions, and improvement strategies. *Renew. Sustain. Energy Rev.* **2023**, *176*, 113208. [CrossRef]
18. Luo, J.; Meng, H.; Yao, Z.; Wachemo, A.C.; Yuan, H.; Zhang, L.; Li, X. Anaerobic co-digestion of sodium hydroxide pretreated sugarcane leaves with pig manure and dairy manure. *Int. J. Agric. Biol.* **2018**, *11*, 224–229. [CrossRef]
19. Castro-Ramos, J.; Solís-Oba, A.; Solís-Oba, M.; Calderón-Vázquez, C.L.; Higuera-Rubio, J.M.; Castro-Rivera, R. Efecto del pH inicial en el proceso de digestión anaeróbica del estiércol de ganado lechero. *AMB Express* **2022**, *12*, 162. [CrossRef] [PubMed]
20. Hasan, S.; Alam, M.; Akter, A.; Uddin, I.; Khaled, M.; Rahman, H. Producción de biogás a partir de residuos de cafetería mediante digestión anaeróbica. In Proceedings of the 2023 5th International Conference on Environment, Resources and Energy Engineering (EREE 2023), Bangkok, Thailand, 15–17 June 2023. [CrossRef]
21. Luo, T.; Zhu, N.; Shen, F.; Long, E.; Long, Y.; Chen, X.; Mei, Z. A Case Study Assessment of the Suitability of Small–Scale Biogas Plants to the Dispersed Agricultural Structure of China. *Waste Biomass Valorization* **2016**, *7*, 1131–1139. [CrossRef]
22. Ibro, M.K.; Ancha, V.R.; Lemma, D.B. Biogas Production Optimization in the Anaerobic Codigestion Process: A Critical Review on Process Parameters Modeling and Simulation Tools. *J. Chem.* **2024**, *1*, 25. [CrossRef]
23. Kegl, T.; Goršek, A.; Pečar, D. Incorporating enriched empirical models into optimization algorithm to enhance biogas production. *Energy* **2025**, *329*, 136706. [CrossRef]
24. Klein, R.; Slaný, V.; Krčálová, E. Conductivity Measurement for Control of a Biogas Plant. *Acta Univ. Agric. Et Silvic. Mendel.* **2018**, *66*, 1151–1156. [CrossRef]
25. Marín-Peña, O.; Alvarado-Lassman, A.; Vallejo-Cantú, N.A.; Juárez-Barojas, I.; Rodríguez-Jarquín, J.P.; Martínez-Sibaja, A. Electrical Conductivity for Monitoring the Expansion of the Support Material in an Anaerobic Biofilm Reactor. *Processes* **2020**, *8*, 77. [CrossRef]
26. Gadirli, G.; Pilarska, A.A.; Dach, J.; Pilarski, K.; Kolasa-Więcek, A.; Borowiak, K. Fundamentals, Operation and Global Prospects for the Development of Biogas Plants—A Review. *Energies* **2024**, *17*, 568. [CrossRef]
27. Wu, D.; Peng, X.; Li, L.; Yang, P.; Peng, Y.; Liu, H.; Wang, X. Commercial biogas plants: Review on operational parameters and guide for performance optimization. *Fuel* **2021**, *303*, 121282. [CrossRef]
28. Wu, D.; Li, L.; Zhen, F.; Liu, H.; Xiao, F.; Sun, Y.; Peng, X.; Li, Y.; Wang, X. Thermodynamics of volatile fatty acid degradation during anaerobic digestion under organic overload stress: The potential to better identify process stability. *Water Res.* **2022**, *214*, 118187. [CrossRef]
29. Wang, K.; Yun, S.; Xing, T.; Li, B.; Abbas, Y.; Liu, X. Binary and ternary trace elements to enhance anaerobic digestion of cattle manure: Focusing on kinetic models for biogas production and digestate utilization. *Bioresour. Technol.* **2021**, *323*, 124571. [CrossRef]

30. Bele, V.; Goyette, B.; An, C.; Anchouri, I.E.; Chaib, O.; Rajagopal, R. Un sistema anaeróbico robusto, de baja temperatura y circuito cerrado para residuos agrícolas mixtos con alto contenido de sólidos: Avances en soluciones de gestión de residuos agrícolas en Canadá. *Environ. Sci. Pollut. Res.* **2024**. [CrossRef]
31. Mata-Alvarez, J.; Macé, S.; Llabrés, P. Anaerobic digestion of organic solid wastes. An overview of research achievements and perspectives. *Bioresour. Technol.* **2000**, *74*, 3–16. [CrossRef]
32. Burg, V.; Bowman, G.; Haubensak, M.; Baier, U.; Thees, O. Valorization of an untapped resource: Energy and greenhouse gas emissions benefits of converting manure to biogas through anaerobic digestion. *Resour. Conserv. Recycl.* **2018**, *136*, 53–62. [CrossRef]
33. Jameel, M.K.; Mustafa, M.A.; Ahmed, H.S.; jassim Mohammed, A.; Ghazy, H.; Shakir, M.N.; Lawas, A.M.; khudhur Mohammed, S.; Idan, A.H.; Mahmoud, Z.H.; et al. Biogas: Production, properties, applications, economic and challenges: A review. *Results Chem.* **2024**, *7*, 101549. [CrossRef]
34. Ahmad, R.M.; Javied, S.; Aslam, A.; Alamri, S.; Zaman, Q.u.; Hassan, A.; Noor, N. Optimizing Biogas Production and Digestive Stability through Waste Co-Digestion. *Sustainability* **2024**, *16*, 3045. [CrossRef]
35. Strömberg, S.; Nistor, M.; Liu, J. Towards eliminating systematic errors caused by the experimental conditions in Biochemical Methane Potential (BMP) tests. *Waste Manag.* **2014**, *34*, 1939–1948. [CrossRef] [PubMed]
36. Kleerebezem, R.; van Loosdrecht, M.C. Mixed culture biotechnology for bioenergy production. *Curr. Opin. Biotechnol.* **2007**, *18*, 207–212. [CrossRef] [PubMed]
37. Raposo, F.; De la Rubia, M.; Fernández-Cegrí, V.; Borja, R. Anaerobic digestion of solid organic substrates in batch mode: An overview relating to methane yields and experimental procedures. *Renew. Sustain. Energy Rev.* **2012**, *16*, 861–877. [CrossRef]
38. Angelidaki, I.; Sanders, W. Assessment of the anaerobic biodegradability of macropollutants. *Rev. Environ. Sci. Biotechnol.* **2004**, *3*, 117–129. [CrossRef]
39. Zhang, L.; Lee, Y.W.; Jahng, D. Anaerobic co-digestion of food waste and piggery wastewater: Focusing on the role of trace elements. *Bioresour. Technol.* **2011**, *102*, 5048–5059. [CrossRef]
40. International Electrotechnical Commission. IEC 60751:2022—webstore.iec.ch; Technical Report; International Electrotechnical Commission: Geneva, Switzerland, 2022. Available online: https://webstore.iec.ch/en/publication/63753 (accessed on 29 September 2025).
41. Aminov, D.; Pines, D.; Kiefer, P.M.; Pines, E. Intact carbonic acid is a viable protonating agent for biological bases. *Proc. Natl. Acad. Sci. USA* **2019**, *116*, 20837–20843. [CrossRef]
42. Tucker, A.M.; Johnson, T.N. Acid-base disorders: A primer for clinicians. *Nutr. Clin. Pract.* **2022**, *37*, 980–989. [CrossRef]
43. Veall, M.R.; Zimmermann, K.F. PSEUDO-R2 Measures for some Common Limited Dependent Variable Models. *J. Econ. Surv.* **1996**, *10*, 241–259. [CrossRef]
44. Shtatland, E.S.; Kleinman, K.; Cain, E.M. One more time about R^2 measures of fit in logistic regression. *NESUG 15 Proc.* **2002**, *15*, 222–226. Available online: https://www.lexjansen.com/nesug/nesug02/st/st004.pdf (accessed on 29 September 2025).
45. Ugba, E.R.; Gertheiss, J. A Modification of McFadden's R^2 for Binary and Ordinal Response Models. *arXiv* **2022**, arXiv:2204.01301. [CrossRef]
46. Liu, D.; Zhu, X.; Greenwell, B.; Lin, Z. A new goodness-of-fit measure for probit models: Surrogate R^2. *Br. J. Math. Stat. Psychol.* **2023**, *76*, 192–210. [CrossRef]
47. Josimović, L.; Prvulović, S.; Djordjević, L.; Bicok, I.; Bakator, M.; Premčevski, V.; Šarenac, U.; Šeljmeši, D. Enhancing Biogas Plant Efficiency for the Production of Electrical and Thermal Energy. *Appl. Sci.* **2024**, *14*, 5858. [CrossRef]
48. Cormos, C.C. Techno-economic and environmental assessment of green hydrogen production via biogas reforming with membrane-based CO_2 capture. *Int. J. Hydrogen Energy* **2025**, *101*, 702–711. [CrossRef]
49. Chen, L.; He, P.; Zou, J.; Zhang, H.; Peng, W.; Lü, F. Scalable and interpretable automated machine learning framework for biogas prediction, optimization, and stability monitoring in industrial-scale dry anaerobic digestion. *Chem. Eng. J.* **2025**, *519*, 165482. [CrossRef]
50. Kegl, T.; Jiménez, E.T.; Kegl, B.; Kralj, A.K.; Kegl, M. Modeling and optimization of anaerobic digestion technology: Current status and future outlook. *Prog. Energy Combust. Sci.* **2025**, *106*, 101199. [CrossRef]
51. Valença, R.B.; dos Santos, L.A.; Firmo, A.L.B.; da Silva, L.C.S.; de Lucena, T.V.; Santos, A.F.d.M.S.; Jucá, J.F.T. Influence of sodium bicarbonate (NaHCO3) on the methane generation potential of organic food waste. *J. Clean. Prod.* **2021**, *317*, 128390. [CrossRef]
52. Su, X.; Shao, X.; Geng, Y.; Tian, S.; Huang, Y. Optimization of feedstock and insulating strategies to enhance biogas production of solar-assisted biodigester system. *Renew. Energy* **2022**, *197*, 59–68. [CrossRef]
53. Li, S.; Ou, X.; Wang, D.; Wang, W. Optimizing biogas production from swine manure: Biogas recirculation coupled with pH adjustment to mitigate lime inhibition. *Process Saf. Environ. Prot.* **2025**, *198*, 107234. [CrossRef]
54. Zeynali, R.; Asadi, M.; Ankley, P.; Mahoney, H.; Brinkmann, M.; Acharya, B.; McPhedran, K.; Soltan, J. Smart municipal wastewater treatment sludge management: Enhancement of biogas production from anaerobic digestion amended by optimized sludge-derived biochar. *Sci. Total Environ.* **2025**, *989*, 179860. [CrossRef] [PubMed]

55. Andole, O.H.; Lei, Z.; Zhang, Z.; Raude, J.; Kanali, C. Optimization of biogas production in dry anaerobic digestion of swine manure by the use of alkalinity index to monitor a prototype cylindrical digester. *Energy* **2017**, *5*, 32–37. [CrossRef]
56. Arslan, M.; Yilmaz, C. Evaluation of multi–hydrogen production for Afyon biogas plant from excess methane and by–product hydrogen sulfide through desulfurization process. *Process Saf. Environ. Prot.* **2025**, *193*, 1139–1156. [CrossRef]
57. Baek, G.; Rossi, R.; Saikaly, P.E.; Logan, B.E. The impact of different types of high surface area brush fibers with different electrical conductivity and biocompatibility on the rates of methane generation in anaerobic digestion. *Sci. Total Environ.* **2021**, *787*, 147683. [CrossRef]
58. Almomani, F.; Bhosale, R.R. Enhancing the production of biogas through anaerobic co-digestion of agricultural waste and chemical pre-treatments. *Chemosphere* **2020**, *255*, 126805. [CrossRef]
59. Baldi, F.; Sdringola, P.; Beozzo, S.; Di Pietra, B. Experimental evaluation and data-driven modelling of a household anaerobic digester for waste-to-biogas conversion. *Renew. Energy* **2025**, *251*, 123333. [CrossRef]
60. Wenjing, T.; Qin, J.; Liu, J.; Liu, F.; Gu, L. Effects of pine sawdust and shrimp shell biochar on anaerobic digestion under different acidification conditions. *J. Environ. Chem. Eng.* **2022**, *10*, 106581. [CrossRef]
61. Weldehans, M.G. Optimization of distillery-sourced wastewater anaerobic digestion for biogas production. *Clean. Waste Syst.* **2023**, *6*, 100118. [CrossRef]
62. Obileke, K.; Makaka, G.; Tangwe, S.; Mukumba, P. Improvement of biogas yields in an anaerobic digestion process via optimization technique. *Environ. Dev. Sustain.* **2024**, *27*, 1–27. [CrossRef]
63. Akar, A.A.; Yousry, E.; Seif, R.; Allam, N.K. Optimizing biogas production with recycled iron nanoparticles: A sustainable approach to anaerobic digestion. *Fuel* **2025**, *386*, 134266. [CrossRef]
64. Pal, S.; Bello, A.; Muratova, E.; Chekanov, A. A review of the materials utilized in the design and fabrication of biogas digesters. *Renew. Sustain. Energy Rev.* **2025**, *211*, 115167. [CrossRef]
65. Mullai, P.; Sambavi, S.; Vishali, S.; Dharmalingam, K.; Sutha, S.; Dinesh, S.; Anandhi, T.; Al Noman, M.A.; Bilyaminu, A.M.; James, A. An integrated review on the role of different biocatalysts, process parameters, bioreactor technologies and data-driven predictive models for upgrading biogas. *J. Environ. Manag.* **2025**, *384*, 125508. [CrossRef]
66. Issahaku, M.; Derkyi, N.S.A.; Kemausuor, F. A systematic review of the design considerations for the operation and maintenance of small-scale biogas digesters. *Heliyon* **2024**, *10*, e24019. [CrossRef]
67. Sarker, S.; Lamb, J.J.; Hjelme, D.R.; Lien, K.M. A review of the role of critical parameters in the design and operation of biogas production plants. *Appl. Sci.* **2019**, *9*, 1915. [CrossRef]